

Fig. (1). (A) Microarray CGH analysis showing deletions at CMT1A/HNPP locus. (B) Schematic presentation of BAC clones delineating the CMT1A/HNPP deletion in the patient. Open circle: BAC clone deleted in the patient, closed circle: BAC clone not deleted in the patient. Closed square: low copy repeat which may have mediated genomic rearrangements. A common 1.4-Mb deletion of HNPP occurs between proximal CMT1A-REP and distal CMT1A-REP. (C,D) BAC FISH analysis in the proband. Arrows show intact signals in 17p11.2 region. Arrow heads show the loss of signal in 17p11.2 region. Clone positions are indicated in Fig. (1B).

## REFERENCES

- [1] MacIntyre DJ, Blackwood DH, Porteous DJ, Pickard BS, Muri WJ. Chromosomal abnormalities and mental illness. *Mol Psychiatry* 2003; 8: 275-87.
- [2] Bassett AS, Chow EW, Weksberg R. Chromosomal abnormalities and schizophrenia. *Am J Med Genet* 2000; 97: 45-51.
- [3] Kunugi H, Lee KB, Nanko S. Cytogenetic findings in 250 schizophrenics: evidence confirming an excess of the X chromosome aneuploidies and pericentric inversion of chromosome 9. *Schizophr Res* 1999; 40: 43-7.
- [4] Millar JK, Wilson-Annan JC, Anderson S, et al. Disruption of two novel genes by a translocation co-segregating with schizophrenia. *Hum Mol Genet* 2000; 9: 1415-23.
- [5] Murphy KC, Owen MJ. The behavioural phenotype in velo-cardio-facial-syndrome. *Am J Hum Genet* 1997; 61: A5.
- [6] Blackwood DH, Fordyce A, Walker MT, St Clair DM, Porteous DJ, Muir WJ. Schizophrenia and affective disorders—co-segregation with a translocation at chromosome 1q42 that directly disrupts brain-expressed genes: clinical and P300 findings in a family. *Am J Hum Genet* 2001; 69: 428-33.
- [7] Lupski JR, de Oca-Luna RM, Slaugenhaupt S, et al. DNA duplication associated with Charcot-Marie-Tooth disease type 1A. *Cell* 1991; 66: 219-232.
- [8] Chance PF, Alderson MK, Leppig KA, et al. DNA deletion associated with hereditary neuropathy with liability to pressure palsies. *Cell* 1993; 72: 143-51.
- [9] Choi BO, Kim J, Lee KL, Yu JS, Hwang JH, Chung KW. Rapid diagnosis of CMT1A duplications and HNPP deletions by multiplex microsatellite PCR. *Mol Cells* 2007; 23: 39-48.
- [10] Wechsler D, translated into Japanese by Shinagawa F, Kobayashi S, Fujita K, Maegawa H. Wechsler Adult Intelligence Scale-Revised Japanese version. SACCESS BELL Co. Ltd., 1990.
- [11] American Psychiatric Association. translated into Japanese by Takahashi S, Ohno Y, Someya T. In Diagnostic and Statistical Manual of Mental Disorders 4th Ed Japanese version. Tokyo: Igaku-Shoin Ltd., 1996.
- [12] First MB, Spitzer RL, Gibbon M, Williams JBW, translated into Japanese by Kitamura T, Okano T. Structured Clinical Interview for DSM-IV Axis I Disorders (SCID) Japanese version. Tokyo: NIPPON HYORONSHA Co. Ltd., 2003.
- [13] Otsubo T, Tanaka K, Koda R, et al. Reliability and validity of Japanese version of the Mini-International Neuropsychiatric Interview. *Psychiatry Clin Neurosci* 2005; 59: 517-526.
- [14] Sheehan DV, Lecrubier Y, Sheehan KH, et al. The Mini-International Neuropsychiatric Interview (M.I.N.I.): the development and validation of a structured diagnostic psychiatric interview for DSM-IV and ICD-10. *J Clin Psychiatry* 1998; 59(Suppl 20): 22-57.
- [15] Miyake N, Shimokawa O, Harada N, et al. BAC array CGH reveals genomic aberrations in idiopathic mental retardation. *Am J Med Genet A* 2006; 140: 205-11.
- [16] Aarskog NK, Vedeler CA. Real-time quantitative polymerase chain reaction. A new method that detects both the peripheral myelin protein 22 duplication in Charcot-Marie-Tooth type 1A disease and the peripheral myelin protein 22 deletion in hereditary neuropathy with liability to pressure palsies. *Hum Genet* 2000; 107: 494-8.
- [17] Mouton P, Tardieu S, Gouider R, et al. Spectrum of clinical and electrophysiologic features in HNPP patients with the 17p11.2 deletion. *Neurology* 1999; 52: 1440-46.
- [18] Dracheva S, Davis KL, Chin B, Woo DA, Schmeidler JH, Aroutunian V. Myelin-associated mRNA and protein expression deficits in the anterior cingulate cortex and hippocampus in elderly schizophrenia patients. *Neurobiol Dis* 2006; 21: 531-40.
- [19] Haroutunian V, Katsel P, Dracheva S, Stewart DG, Davis KL. Variations in oligodendrocyte-related gene expression across multiple cortical regions: implications for the pathophysiology of schizophrenia. *Int J Neuropsychopharmacol* 2007; 10: 565-73.
- [20] Davis KL, Stewart DG, Friedman JI, et al. White matter changes in schizophrenia: evidence for myelin-related dysfunction. *Arch Gen Psychiatry* 2003; 60: 443-56.
- [21] Hakak Y, Walker JR, Li C, et al. Genome-wide expression analysis reveals dysregulation of myelination-related genes in chronic schizophrenia. *Proc Natl Acad Sci USA* 2001; 98: 4746-51.
- [22] Vostrikov VM, Uranova NA, Orlovskaya DD. Deficit of perineuronal oligodendrocytes in the prefrontal cortex in schizophrenia and mood disorders. *Schizophr Res* 2007; 94: 273-80.
- [23] Roy K, Murrie JC, El-Khodori BF, et al. Loss of erbB signaling in oligodendrocytes alters myelin and dopaminergic function, a potential mechanism for neuropsychiatric disorders. *Proc Natl Acad Sci USA* 2007; 104: 8131-6.
- [24] Shergill SS, Kanaan RA, Chitnis XA, et al. A diffusion tensor imaging study of fasciculi in schizophrenia. *Am J Psychiatry* 2007; 164: 467-73.
- [25] Dougherty KD, Dreyfus CF, Black IB. Brain-derived neurotrophic factor in astrocytes, oligodendrocytes, and microglia/macrophages after spinal cord injury. *Neurobiol Dis* 2000; 7: 574-85.
- [26] Deadwyler GD, Pouly S, Antel JP, Devries GH. Neuregulins and erbB receptor expression in adult human oligodendrocytes. *Glia* 2000; 32: 304-12.
- [27] Hashimoto T, Lewis DA. BDNF Val66Met polymorphism and GAD67 mRNA expression in the prefrontal cortex of subjects with schizophrenia. *Am J Psychiatry* 2006; 163: 534-7.
- [28] Stefansson H, Sigurdsson E, Steinthorsdottir V, et al. Neuregulin 1 and susceptibility to schizophrenia. *Am J Hum Genet* 2002; 71: 877-92.
- [29] Bulayeva KB, Glatt SJ, Bulayeva OA, Pavlova TA, Tsuang MT. Genome-wide linkage scan of schizophrenia: a cross-isolate study. *Genomics* 2007; 89: 167-77.
- [30] Bulayeva KB, Leal SM, Pavlova TA, et al. Mapping genes of complex psychiatric diseases in Daghestan genetic isolates. *Am J Med Genet B Neuropsychiatr Genet* 2005; 132: 76-84.
- [31] Williams NM, Norton N, Williams H, et al. A systematic genome-wide linkage study in 353 sib pairs with schizophrenia. *Am J Hum Genet* 2003; 73: 1355-67.

Supportive evidence for reduced expression of *GNBIL* in schizophrenia

Hiroki Ishiguro<sup>1-3</sup>, Minoru Koga<sup>2,3</sup>, Yasue Horiuchi<sup>2,3</sup>, Emiko Noguchi<sup>2</sup>, Miyuki Morikawa<sup>2</sup>, Yoshimi Suzuki<sup>2</sup>, Makoto Arai<sup>4</sup>, Kazuhiro Niizato<sup>5</sup>, Shyuji Iritani<sup>5</sup>, Masanari Itokawa<sup>3,5</sup>, Toshiya Inada<sup>6</sup>, Nakao Iwata<sup>7</sup>, Norio Ozaki<sup>8</sup>, Hiroshi Ujike<sup>9</sup>, Hiroshi Kunugi<sup>10</sup>, Tsukasa Sasaki<sup>11</sup>, Makoto Takahashi<sup>12</sup>, Yuichiro Watanabe<sup>12</sup>, Toshiyuki Someya<sup>12</sup>, Akiyoshi Kakita<sup>13</sup>, Hitoshi Takahashi<sup>14</sup>, Hiroyuki Nawa<sup>15</sup>, and Tadao Arinami<sup>2,3</sup>

<sup>1</sup>Department of Medical Genetics, Graduate School of Comprehensive Human Sciences, University of Tsukuba, Tsukuba, Ibaraki 305-8577, Japan; <sup>2</sup>CREST, Japan Science and Technology Agency, Kawaguchi-shi, Saitama 332-0012, Japan; <sup>3</sup>Department of Schizophrenia Research, Tokyo Institute of Psychiatry, Tokyo 156-8585, Japan; <sup>4</sup>Tokyo Metropolitan Matsuzawa Hospital, Department of Psychiatry, Tokyo 156-0057, Japan; <sup>5</sup>Seiwa Hospital, Institute of Neuropsychiatry, Tokyo 162-0851, Japan; <sup>6</sup>Department of Psychiatry, Fujita Health University School of Medicine, Toyoake, Aichi 470-1192, Japan; <sup>7</sup>Department of Psychiatry, Nagoya University, School of Medicine, Nagoya 466-8550, Aichi, Japan; <sup>8</sup>Department of Neuropsychiatry, Okayama University, Graduate School of Medicine, Dentistry and Pharmaceutical Sciences, 2-5-1 Shikata-cho, Okayama 700-8558, Japan; <sup>9</sup>National Center of Neurology and Psychiatry, Tokyo 187-8551, Japan; <sup>10</sup>Health Service Center, University of Tokyo, Tokyo 113-0033, Japan; <sup>11</sup>Department of Psychiatry, Niigata University Graduate School of Medical and Dental Sciences, Niigata 951-8510, Japan; <sup>12</sup>Brain Research Institute, Niigata University, Niigata 951-8585, Japan, Department of Pathology; <sup>13</sup>Department of Pathological Neuroscience, Brain Research Institute, Niigata University, Niigata 951-8585, Japan; <sup>14</sup>Department of Pathology, Brain Research Institute, Niigata University, Niigata 951-8585, Japan

**Background:** Chromosome 22q11 deletion syndrome (22q11DS) increases the risk of development of schizophrenia more than 10 times compared with that of the general population, indicating that haploinsufficiency of a subset of the more than 20 genes contained in the 22q11DS region could increase the risk of schizophrenia. In the present study, we screened for genes located in the 22q11DS region that are expressed at lower levels in postmortem prefrontal cortex of patients with schizophrenia than in those of con-

trols. **Methods:** Gene expression was screened by Illumina Human-6 Expression BeadChip arrays and confirmed by real-time reverse transcription-polymerase chain reaction assays and Western blot analysis. **Results:** Expression of *GNBIL* was lower in patients with schizophrenia than in control subjects in both Australian (10 schizophrenia cases and 10 controls) and Japanese (43 schizophrenia cases and 11 controls) brain samples. *TBX1* could not be evaluated due to its low expression levels. Expression levels of the other genes were not significantly lower in patients with schizophrenia than in control subjects. Association analysis of tag single-nucleotide polymorphisms in the *GNBIL* gene region did not confirm excess homozygosity in 1918 Japanese schizophrenia cases and 1909 Japanese controls. Haloperidol treatment for 50 weeks increased *Gnb1l* gene expression in prefrontal cortex of mice. **Conclusions:** Taken together with the impaired prepulse inhibition observed in heterozygous *Gnb1l* knockout mice reported by the previous study, the present findings support assertions that *GNBIL* is one of the genes in the 22q11DS region responsible for increasing the risk of schizophrenia.

**Key words:** 22q11DS/haloperidol/prefrontal cortex/postmortem brain

## Introduction

Schizophrenia, a devastating mental disorder that affects approximately 1% of the world's population, is a genetically complex disorder. The multifactorial polygenic model has received the most support as the mode of inheritance that underlies the familial distribution of schizophrenia; therefore, a variety of genetic, environmental, and stochastic factors are likely involved in the etiology. However, it is also possible that specific genes play major roles in susceptibility to schizophrenia. Genes involved in 22q11.2 deletion syndrome (22q11DS) substantially increases susceptibility to schizophrenia. 22q11DS is associated with several diagnostic labels including DiGeorge syndrome, velocardiofacial (or Shprintzen) syndrome (VCFS), conotruncal anomaly face, Cayler syndrome, and Opitz GBBB syndrome. Schizophrenia is a late manifestation in approximately 30% of 22q11DS cases, which is comparable to the risk to offspring of 2 parents with schizophrenia. The 22q11 deletion is detected relatively frequently in patients with schizophrenia;

<sup>1</sup>To whom correspondence should be addressed; Department of Medical Genetics, Graduate School of Comprehensive Human Sciences, University of Tsukuba, 1-1-1 Tennoudai, Tsukuba, Ibaraki 305-8575, Japan; tel: +81-29-853-3352, fax: +81-29-853-3333, e-mail: hishigur@md.tsukuba.ac.jp

a number of studies have shown that 22q11DS schizophrenia is a true genetic subtype of schizophrenia<sup>1,2</sup>.

Although the deleted region is approximately 3 Mbp in most patients with 22q11DS, the critical region is approximately 1.5 Mbp.<sup>3,4</sup> Less than 30 genes are located in the 22q11DS region. Studies of 22q11DS patients without the common chromosomal deletion suggested that the *TBX1* is a major contributor to the conotruncal malformations of 22q11DS.<sup>5</sup> One of the mutations in the *TBX1* was found to be a loss-of-function mutation.<sup>6</sup> Mice heterozygous for a null mutation in *Tbx1* develop conotruncal defects.<sup>7</sup> Deletion of one copy of the *Tbx1* affects the development of the fourth pharyngeal arch arteries, whereas the homozygous mutation severely disrupts the pharyngeal arch artery system.<sup>8</sup> The contribution of the *TBX1* haploinsufficiency to psychiatric disease was suggested by the identification of a family with VCFS in a mother and her 2 sons. These 3 patients all had a null mutation of the *TBX1*, and one of the sons was diagnosed with Asperger syndrome after psychiatric assessment.<sup>9</sup>

Contribution of genes in the 22q11DS region to susceptibility to schizophrenia has been examined mainly by genetic association studies. Associations between schizophrenia and nucleotide variations in the *ZNF74*,<sup>10</sup> *DGCR*,<sup>11</sup> *DGCR14*,<sup>12</sup> *PRODH*,<sup>13</sup> *ZDHHC8*,<sup>14</sup> *COMT*,<sup>15-18</sup> and *CLDN5*<sup>19,20</sup> genes have been reported. These associations, however, have not been confirmed in other populations<sup>19-22</sup> or by meta-analyses.<sup>19-24</sup>

Studies of genetically engineered mice have provided supporting evidence for roles of the genes located in the human 22q11DS region in schizophrenia. *Prodh* knockout mice exhibited deficits in learning and responses to psychomimetic drugs.<sup>25</sup> Observation of overlapping loci across 5 heterozygous mice strains with different deletion sites revealed that a 300-kb locus, which contains the *Gnb11*, *Tbx1*, *Gplbb*, and *Sept5* genes, is crucial for impaired sensorimotor gating measured by prepulse inhibition test (PPI).<sup>9</sup> In that study, the authors speculated that the *GPIBB* was unlikely to be related to schizophrenia because it is expressed only in platelets. The *GPIBB* causes Bernard-Soulier disease, which has no associated psychiatric disorders. The *Sept5* heterozygous knockout mice did not show impaired PPI. *Gnb11* or *Tbx1* heterozygous knockout mice showed reduced PPI.<sup>9</sup> Therefore, the authors concluded that the *Tbx1* and *Gnb11* are strong candidates for psychiatric disease in patients with 22q11DS.<sup>9</sup> In another study, however, *Tbx1* heterozygous knockout mice showed normal locomotor activity, habituation, nesting, and locomotor responses to amphetamine.<sup>25</sup>

Recently, Williams et al.<sup>26</sup> reported associations between polymorphisms in the *GNBIL* gene region and schizophrenia in the United Kingdom, German, and Bulgarian population. They found excess homozygosity at rs5746832 and rs2269726 in male schizophrenia subjects and that the markers associated with male schizophrenia were related with cis-acting changes in *GNBIL* expres-

sion. These mouse and human studies indicated a correlation between *GNBIL* gene expression and psychosis.

The working hypothesis of the present study was that genes in the 22q11DS region involved in the susceptibility to schizophrenia were likely to be expressed at lower levels in patients with schizophrenia than in control subjects. We performed a scan of expressional changes of the genes in the 22q11DS region in schizophrenic and control prefrontal cortex and found that the *GNBIL* gene was compatible with our hypothesis.

## Materials and methods

### Human Postmortem Brains

Brain specimens were from individuals of European descent Australian and Japanese. Australian sample comprised 10 schizophrenic patients and 10 age- and gender-matched controls (Supplementary Table S1). The diagnosis of schizophrenia was made according to the Diagnostic and Statistical Manual of Mental Disorders (DSM)-IV criteria (American Psychiatric Association 1994) by a psychiatrist and a senior psychologist. Control subjects had no known history of psychiatric illness. Tissue blocks were cut from gray matter in an area of the prefrontal cortex referred to as Brodmann's area 9 (BA9). Japanese samples of BA9 gray matter from Japanese brain specimens consisted of 6 schizophrenic patients and 11 age- and gender-matched controls (Supplementary Table S1). In addition, postmortem brains of 37 deceased Japanese patients with schizophrenia were also analyzed (Supplementary Table S1). The Japanese subjects met the DSM-III-R criteria for schizophrenia. The study was approved by the Ethics Committees of Central Sydney Area Health Service, University of Sydney, Niigata University, University of Tsukuba, Tokyo Metropolitan Matsuzawa Hospital, and Tokyo Institute of Psychiatry.

### RNA Isolation and Gene Expression Microarray

Total RNA was extracted from brain tissues with ISOGEN Reagent (Nippon Gene Co, Tokyo, Japan). The RNA quality was checked using a Nanodrop ND-1000 spectrophotometer (LMS, Tokyo, Japan) to have an OD 260/280 ratio of 1.8-2 and an OD 260/230 of 1.8 or greater. Microarrays were used to screen for differential gene expression between Australian schizophrenic patients and controls. In brief, 500 ng of total RNAs were reverse transcribed to synthesize first- and second-strand complementary DNA (cDNA), purified with spin columns, then in vitro transcribed to synthesize biotin-labeled complementary RNA (cRNA). A total of 1500 ng of biotin-labeled cRNA was hybridized on Sentrix® Human-6 Expression BeadChip (Illumina Inc., San Diego, CA) at 55°C for 18 h. The hybridized BeadChip was washed and labeled with streptavidin-Cy3, then scanned with an Illumina BeadStation 500 System

(Illumina Inc). Scanned image was imported into BeadStudio (Illumina Inc) for analysis. Forty-six thousand transcripts can be analyzed by a single BeadChip.

#### Real-time Quantitative RT-polymerase chain reaction

Expression of the *GSCL*, *HIRA*, *SEPT5*, *GNB1L*, *TBX1*, and *CDC45L* genes was analyzed by TaqMan Real-time polymerase chain reaction (PCR) system (Applied Biosystems, Foster City, CA). From RNA, cDNA was synthesized with Revertra Ace (Toyobo, Tokyo, Japan) and oligo dT primer. Expression of these 6 genes was analyzed with an ABI PRISM 7900 HT Sequence Detection System (Applied Biosystems), with the TaqMan gene expression assays for *GSCL* (Hs00232019\_m1), *HIRA* (Hs00983699\_m1), *SEPT5* (Hs00160237\_m1), *GNB1L* (Hs00223722\_m1), *TBX1* (Hs00271949\_m1), and *CDC45L* genes (Hs00185895\_m1) and normalized to expression of Human *GAPDH* Control Reagents (Applied Biosystems). *GNB1L* expression was analyzed in Australian samples and replicated the analysis in Japanese subjects.

#### Protein Isolation and GNB1L Protein Levels in Brain

Protein was extracted from prefrontal cortex tissues with Laemmli Buffer. Western blotting method was used to compare GNB1L protein levels between schizophrenics and controls. Each of 2  $\mu$ g protein was run on Pro-Pure™ SPRINT NEXT GEL (Amresco, Solon, OH) and transferred to BioTrace™ PVDF (Nihon Pall Ltd, Tokyo, Japan). Polyclonal antibodies against the human GNB1L protein (OTTHUMP00000028644) were generated by injecting rabbits with the following peptide: CAGSKDQ-RISLWSLYPRA (MBL, Nagoya, Japan). Mouse polyclonal antibody against beta-actin (Sigma Aldrich Japan, Tokyo, Japan) was also used for normalization purpose. The bound primary antibodies were detected with goat anti-rabbit or anti-mouse IgG antibody HRP conjugate (MBL) and Immobilon™ Western, Chemiluminescent HRP Substrate (Millipore, Billerica, MA) on X-film (Fujifilm Medical, Tokyo, Japan). The signals of GNB1L or beta-actin of each subject on X-films were quantitated by computer software, ImageJ 1.40g (<http://rsb.info.nih.gov/ij/>), and GNB1L protein levels were normalized to beta-actin and compared.

#### Peripheral Blood and Brain DNA Sample and Genotyping

The subjects comprised 1918 unrelated Japanese patients with schizophrenia (1055 men, 863 women; mean age  $\pm$  standard deviation [SD], 48.9  $\pm$  14.5 years) diagnosed according to DSM-IV with consensus from at least 2 experienced psychiatrists and 1909 mentally healthy unrelated Japanese control subjects (1012 men, 893 women; mean age  $\pm$  SD, 49.0  $\pm$  14.3 years) of whom the first- and second-degree relatives were free of psychosis as self-reported by the subjects. The association analysis

was approved by the Ethics Committees of the University of Tsukuba, Niigata University, Fujita Health University, Nagoya University, Okayama University, and Teikyo University, National Center of Neurology and Psychiatry, University of Tokyo, and all participants provided written informed consent. DNAs were extracted from these blood samples and the same brain tissues used for gene expression analysis. The tag single-nucleotide polymorphisms (SNPs) comprising rs5746832, rs5746834, rs2269726, rs748806, rs29807124, rs5993835, rs13057609, rs4819523, rs2073765, rs7286924, rs10372, rs3788304, and rs11704083 at the *GNB1L* gene region were selected by Haploview program using HapMap Project Japanese data set (<http://www.hapmap.org/>), as the previously reported schizophrenia-associated SNPs, rs5746832 and rs2269726, were forced included. The TaqMan reaction was performed in a final volume of 3  $\mu$ l consisting of 2.5 ng genomic DNA and Universal Master Mix (EUROGENTEC, Seraing, Belgium), and genotyping was performed with an ABI PRISM 7900HT Sequence Detection System (Applied Biosystems).

Genotyping quality control consisted of  $\geq$ 98% successful calls. We confirmed concordance among repeat genotyping in  $\approx$ 10% of genotypes.

#### Brain GNB1L Expression and Genotyping

The correlations between *GNB1L* expression and 13 SNPs, rs5746832, rs5746834, rs2269726, rs748806, rs29807124, rs5993835, rs13057609, rs4819523, rs2073765, rs7286924, rs10372, rs3788304, and rs11704083, were examined in Australian and Japanese brain tissues, respectively.

#### Mice Experiments

Mice treated with haloperidol were studied to examine the effects of antipsychotic treatments on *Gnb1l* gene expression. Thirty-nine C57/BJ6 male mice (age, 8 weeks; weight, 20–25 g) were housed under 10 h/14 h light/dark conditions with normal food and water ad libitum, where groups of 5 or 6 mice were housed separately, and 0.5 mg/kg haloperidol or saline was injected intraperitoneally once each day for 4 weeks or for 50 weeks. The dosage of haloperidol was at maximum clinically used, and 4 or 50 weeks for treatment term correspond to several years or half a lifetime in human terms, respectively. We used extreme but likely condition to clear up the effect of the medication. We determined the dosage of haloperidol according to the previous studies.<sup>27–31</sup> Mice were sacrificed 4 h after the last injection to obtain brain tissues.

The prefrontal cortex was taken, and RNA was extracted with RNeasy kit (Qiagen, K.K., Tokyo, Japan). A cDNA was synthesized with Revertra Ace (Toyobo) and oligo dT primer. Expression of *Gnb1l* was analyzed by TaqMan real-time polymerase chain reaction (PCR) with an ABI PRISM 7900 HT Sequence Detection System (Applied Biosystems), with the TaqMan gene expression assay for *Gnb1l* (Mm00499153\_m1). Expression of

*Gnb1l* was normalized to that of rodent *Gapdh* with Rodent *Gapdh* Control Reagents (Applied Biosystems).

All animal procedures were performed according to protocols approved by the Animal Care and Use committee of University of Tsukuba.

#### Statistics

Microarray analysis was performed with GeneSpring software version 7.3.1 (Silicon Genetics, Redwood, CA). The mean background noise level was first corrected in each sample, and then per-chip normalization was applied to eliminate systematic differences between chips. Two-tailed Student's *t*-test was used to examine the difference between schizophrenic patients and controls. In real-time PCR experiments, *GAPDH* or *Gapdh* was used as an internal control, and measurement of threshold cycle (Ct) was performed in triplicate. Data were collected and analyzed with Sequence Detector Software version 2.1 (Applied Biosystems) and the standard curve method. Relative gene expression was calculated as the ratio of expression of the target gene to the internal control (*GAPDH* or *Gapdh*). Correlations of *GNB1L* gene expressions and 2 quality parameters, postmortem interval (PMI) and pH, of brain samples were analyzed with analysis of variance (ANOVA) one-way tests by JMP computer software version 5.1. The density of images reflecting *GNB1L* protein levels was also compared between schizophrenics and controls with the Wilcoxon test implemented in JMP computer software version 5.1. Deviation from Hardy-Weinberg equilibrium (HWE), allelic associations, and linkage disequilibrium (LD) between SNPs were evaluated with Haploview software version 3.11. A nominal association was defined when the given *P* value for allelic or genotypic tests was less than 5% (uncorrected  $P < .05$ ). If a nominal significant association was found in the analysis, permutation test was also performed with Haploview software version 3.11. Correlations of *GNB1L* gene expressions and either protein expression or genotypes of the tag SNPs were analyzed with ANOVA one-way tests by JMP computer software version 5.1.

#### Results

Human-6 Expression BeadChip demonstrated that *GSC1L* (GI\_48885362-S) and *TBX1* (GI\_18104949-I) of 28 genes located in the 22q11DS region were expressed at lower levels in schizophrenic brains than in the control brains in the Australian samples ( $P < .05$ ) (Supplementary Table S2). However, the signals of these transcripts were low, and reliable confidence was not obtained from any subject. Expression of *CDC45L* (GI\_34335230-S) tended to be lower in schizophrenic brains than in control brains ( $P = .07$ ). Data of *GNB1L* were not available in this platform (Supplementary Table S2).

We used real-time PCR experiments to evaluate expression of the 3 genes that were potentially underexpressed in schizophrenia prefrontal cortex by microarray and *GNB1L*, which was not assessed by the microarray in the Australian and Japanese brain samples. The difference in gene expression between the schizophrenia and control groups was not confirmed for *CDC45L*. In addition, because the reliability of *HIRA* and *SEPT5* was not sufficient due to weakly expressed sequences in the array screening, we reexamined expression levels of these genes by real-time PCR method and did not find significant differences in gene expression between the schizophrenia and control groups. Expressions of *TBX1* and *GSC1L* were too low to obtain reliable signals with the TaqMan gene expression assay (Hs00271949\_m1 and Hs00232019\_m1, respectively). Relative expression of *GNB1L* was significantly lower in Australian schizophrenic prefrontal brains than in Australian control brains (average ratio = 0.57,  $P < .001$ ) and in Japanese patients with schizophrenia than in control subjects (average ratio = 0.53,  $P < .0001$ ) (figure 1A). No difference in *GNB1L* expression was observed between the Japanese and Australian schizophrenic patient groups (data not shown). *GNB1L* expression was not significantly correlated with pH of the brain tissue samples overall (figure 2), neither with gender ( $P = .62$ ) nor PMI ( $F = 0.61$ ,  $P = .44$ ). Western blotting analysis also demonstrated the lower levels of *GNB1L* protein in brains of the schizophrenia sample than in those of the control sample from each ethnic group (approximate average ratio = 0.75,  $P = .027$  in Australian sample and approximate average ratio = 0.69,  $P = .033$  in Japanese sample) (figure 1B). There is a significant correlation between gene and protein expression observed in our samples ( $F = 4.7$ ,  $P = .037$ ).

There were no significant associations of tag SNPs at the *GNB1L* gene studied in the present study with schizophrenia in our Japanese case-control sample (table 1). Also no significant differences were found in distributions of homozygotes and heterozygotes between schizophrenics and controls (table 1). Williams et al.<sup>26</sup> reported male-specific associations of rs5746832 and rs2269726 with schizophrenia and correlation between those markers and the gene expression. However, such male-specific associations of rs5746832 and rs2269726 were not observed in our sample (table 1).

There was a nominally significant correlation between rs5748832 and *GNB1L* expressions in whole subjects ( $P = .014$ ) and in Japanese ( $P = .028$ ), but not in Australian ( $P = .66$ ) (table 2). An allele of rs5748832 is correlated with high *GNB1L* expression in this study, while the previous study showed the opposite direction of correlation.<sup>26</sup>

Significant deviation from HWE in the genotypic distributions was observed at rs4819523 in the control group. Lower proportions of heterozygotes than those expected by HWE seemed to cause these deviations. Although genotype errors, chance findings, or actual

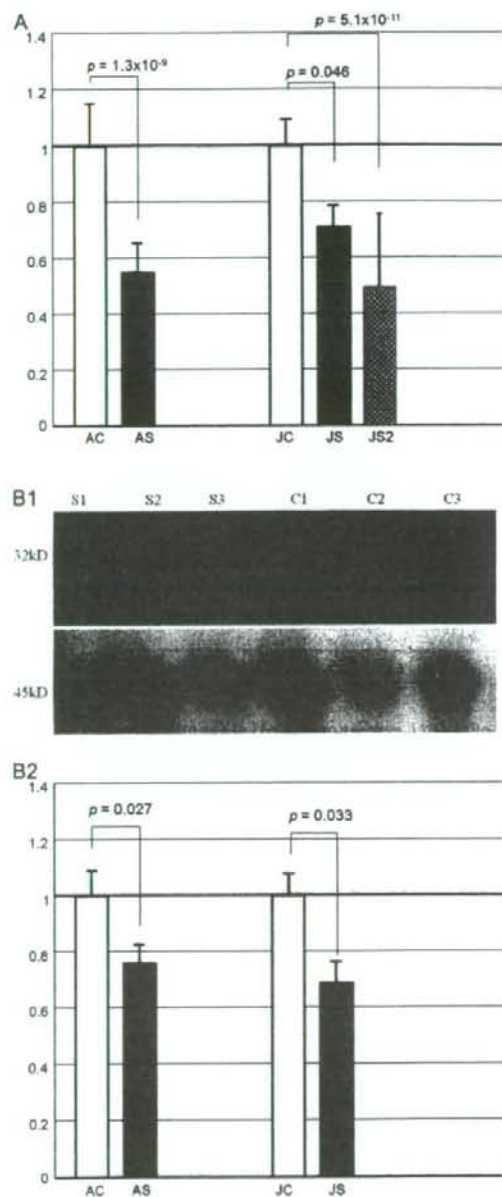


Fig. 1. GNB1L expression in schizophrenic brain (A). Relative expression of the *GNB1L* gene in prefrontal cortex from Australian control subjects (AC,  $n = 10$ ), Australian schizophrenics (AS,  $n = 10$ ), Japanese controls (JC,  $n = 11$ ), Japanese schizophrenics (JS,  $n = 6$ ), and additional Japanese schizophrenics (JS2,  $n = 37$ ). The vertical scores show average of relative expression and  $\pm 1$  SD in comparison with control subjects in each ethnic population, respectively. (B-1) A partial result of Western blotting was shown. Upper: GNB1L (Although expected size would be 35 kD, bands are expressed at 32 kD according to the antibody protocol) Lower: beta

structural variations in some subjects might have potentially caused these deviations, we could not determine which was most likely to cause these HWE deviations.

*Gnb1l* expression in mice was examined to exclude the possibility that reduced *GNB1L* expression was the effects of chronic treatment with antipsychotic drugs. The patients whose brains were examined in the present study had received long-term medication of typical antipsychotic drugs; therefore, we chose haloperidol as a representative antipsychotic drug. As a result, while *Gnb1l* gene expression in prefrontal cortex of mice treated with haloperidol for 4 weeks was not changed, the expression was higher in those treated with haloperidol for 50 weeks than in those with saline injected ( $P = .02$ ) as shown in figure 3.

## Discussion

In the present study, we hypothesized that haploinsufficiency of some genes in the 22q11DS region might increase the susceptibility to schizophrenia not only in patients with 22q11DS but also in the those without 22q11DS and that such genes would be expressed at lower levels in the brains of schizophrenic patients than in control subjects. *GNB1L* appears to meet this hypothesis. Reduced *GNB1L* gene expression was detected in both mRNA and protein levels in Australian and Japanese subjects, suggesting that lower *GNB1L* gene expression produces lower GNB1L protein levels which underlie schizophrenia across ethnicities. Treatment of mice with haloperidol indicated that the reduction of *GNB1L* expression is not likely a consequence of antipsychotic medication treatment, though the possibility of reduction of *GNB1L* expression by other antipsychotic drugs remains. The present study did not provide evidence of whether *TBX1* expression is altered significantly in schizophrenic brains because the signals detected by Illumina's Sentrix® Human-6 Expression BeadChip or TaqMan assay were very weak. Paylor et al<sup>9</sup> mapped PPI deficits in a panel of mouse mutants and found that PPI was impaired by either haploinsufficiency of *Tbx1* or *Gnb1l*. The present study of human brains confirms that *GNB1L* is an important candidate for susceptibility to schizophrenia.

There is little information about the function of GNB1L. *GNB1L* expression is relatively low in adult brain but is high in fetal brain. *GNB1L* encodes a guanine

actin (45 kD). Samples S1–S3 are from schizophrenic patients and C1–C3 are from controls. (B-2) Relative expression of the GNB1L protein in prefrontal cortex from Australian control subjects (AC,  $n = 10$ ), Australian schizophrenics (AS,  $n = 10$ ), Japanese controls (JC,  $n = 11$ ), and Japanese schizophrenics (JS,  $n = 6$ ). The vertical scores show average of relative expression and  $\pm 1$  SD in comparison with control subjects in each ethnic population, respectively.

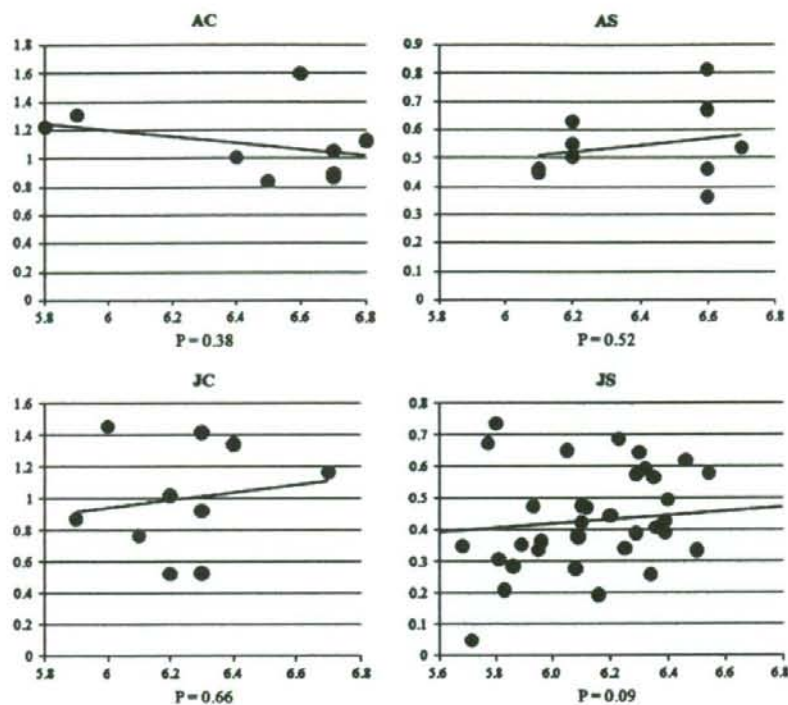


Fig. 2. *GNB1L* expression and pH in human postmortem brain. Correlation of *GNB1L* expression and pH of the human postmortem brain subjects used in the same experiments shown in figure 1; AC, Australian controls; AS, Australian schizophrenics; JC, Japanese controls; JS, Japanese schizophrenics; JS2, additional Japanese schizophrenic samples. The vertical scale shows relative *GNB1L* expression and horizontal scale shows pH. Statistical *P* values are calculated below each graph.

nucleotide-binding protein (G protein), beta polypeptide 1-like, which is a member of the WD repeat protein family. WD repeats are minimally conserved regions of approximately 40 amino acids typically bracketed by Gly-His and Trp-Asp (GH-WD) that may facilitate formation of heterotrimeric or multiprotein complexes. Members of this family are involved in a variety of cellular processes, including cell cycle progression, signal transduction, apoptosis, and gene regulation. *GNB1L* contains 6 WD repeats.<sup>32</sup> *GNB1L* shows homology to the human guanine nucleotide-binding protein  $\beta$  subunit (*GNB1*). *GNB1* functions in G-protein-coupled receptor protein signaling pathways and intracellular signaling cascade.

Williams et al.<sup>26</sup> reported excess homozygosity at rs5746832 and rs2269726 in male schizophrenia subjects and that the markers associated with male schizophrenia were related with cis-acting changes in *GNB1L* expression. Firstly in the present study, we failed to confirm the association in our Japanese case-control population. Secondly, we found a nominally significant correlation between rs5746832 and *GNB1L* expression in the Japanese brain samples, but failed to find it in our limited number

of the Australian samples. Further, the association between allele and gene expression in our Japanese samples was in the opposite direction from that reported in the Caucasian samples. It might be due to possible differences in LD block between haplotype phases across rs5746832 and harboring potential cis-acting variations of the gene between 2 ethnic populations. Even if such cis-acting variations are present, diagnosis has tremendous effect on the gene expression, in comparison to that of the SNP. The power of the present study to replicate the findings of excess homozygosity in male subjects is greater than 90% assuming the odd ratio of greater than 1.5 found in UK populations by Williams et al.<sup>26</sup> However, if the odd ratio assumes 1.3 observed in a German population by them, the power drops to 0.65. Although the gene frequencies of rs5746832 and rs2269726 were significantly different between Caucasian and Japanese populations, the frequencies of homozygotes were almost the same between 2 populations. Because of small sample size, we did not attempt allele-specific expression analysis in our brain sample. Therefore, we could not conclude whether lower *GNB1L* gene/protein expression in schizophrenia was



Table 1. Analysis of Tag Single-Nucleotide Polymorphisms at the GNBIL Gene in the Japanese Case-Control Population

Population	Genotype count (frequency)			HWE P	Allele count (frequency)			P	Homozygote	Heterozygote	P
	AA	AG	GG		A	G					
rs746832											
Affected	n = 1889	501 (0.27)	958 (0.51)	430 (0.23)	1960 (0.52)	1818 (0.48)		931 (0.49)	958 (0.51)		
Male only	n = 1008	256 (0.25)	531 (0.53)	221 (0.22)	1884 (0.50)	1868 (0.50)		477 (0.47)	531 (0.53)		
Controls	n = 1876	484 (0.26)	916 (0.49)	476 (0.25)	1876 (0.50)	1876 (0.50)		960 (0.51)	916 (0.49)	.24	
Male only	n = 1047	260 (0.25)	524 (0.50)	263 (0.25)	1876 (0.50)	1876 (0.50)		523 (0.50)	524 (0.50)	.23	
rs746834											
Affected	n = 1898	1652 (0.87)	234 (0.12)	12 (0.01)	3538 (0.93)	258 (0.07)	T	1664 (0.88)	234 (0.12)		
Controls	n = 1893	1653 (0.87)	228 (0.12)	12 (0.01)	3534 (0.93)	252 (0.07)	T	1665 (0.88)	228 (0.12)	.77	
rs2269726											
Affected	n = 1905	338 (0.18)	896 (0.47)	671 (0.35)	1572 (0.41)	2238 (0.59)	C	1009 (0.53)	896 (0.47)		
Male only	n = 1050	176 (0.17)	51 (0.49)	363 (0.35)	1572 (0.41)	2238 (0.59)	C	539 (0.51)	511 (0.49)		
Controls	n = 1906	309 (0.16)	911 (0.48)	686 (0.36)	1529 (0.40)	2283 (0.60)	C	995 (0.52)	911 (0.48)	.65	
Male only	n = 1042	174 (0.17)	49 (0.48)	370 (0.36)	1529 (0.40)	2283 (0.60)	C	544 (0.52)	498 (0.48)	.69	
rs748806											
Affected	n = 1888	537 (0.28)	919 (0.49)	432 (0.23)	1993 (0.53)	1783 (0.47)	C	969 (0.52)	919 (0.48)		
Controls	n = 1895	526 (0.28)	911 (0.48)	458 (0.24)	1963 (0.52)	1827 (0.48)	C	984 (0.51)	911 (0.49)	.72	
rs29807124											
Affected	n = 1872	1688 (0.90)	177 (0.09)	7 (0.00)	3553 (0.95)	191 (0.05)	G	1695 (0.91)	177 (0.09)		
Controls	n = 1873	1693 (0.90)	174 (0.09)	6 (0.00)	3560 (0.95)	186 (0.05)	G	1699 (0.90)	174 (0.10)	.82	
rs593835											
Affected	n = 1881	1474 (0.78)	374 (0.20)	33 (0.02)	3322 (0.88)	440 (0.12)	G	1507 (0.80)	374 (0.20)		
Controls	n = 1871	1484 (0.79)	365 (0.20)	22 (0.01)	3333 (0.89)	409 (0.11)	G	1506 (0.80)	365 (0.20)	.77	
rs13057609											
Affected	n = 1888	13 (0.01)	271 (0.14)	1604 (0.85)	297 (0.08)	3479 (0.92)	G	1617 (0.86)	271 (0.14)		
Controls	n = 1883	10 (0.01)	272 (0.14)	1601 (0.85)	292 (0.08)	3474 (0.92)	G	1611 (0.86)	272 (0.14)	.93	
rs4819523											
Affected	n = 1886	536 (0.28)	932 (0.49)	418 (0.22)	2004 (0.53)	1768 (0.47)	C	954 (0.51)	932 (0.49)		
Controls	n = 1896	562 (0.30)	887 (0.47)	447 (0.24)	2011 (0.53)	1781 (0.47)	C	1009 (0.53)	887 (0.47)	.10	
rs2073765											
Affected	n = 1887	90 (0.05)	586 (0.31)	1211 (0.64)	766 (0.20)	3008 (0.80)	T	1301 (0.69)	586 (0.31)		
Controls	n = 1895	76 (0.04)	590 (0.31)	1229 (0.65)	742 (0.20)	3048 (0.80)	T	1305 (0.69)	590 (0.31)	.97	
rs7286924											
Affected	n = 1892	808 (0.43)	848 (0.45)	236 (0.12)	2464 (0.65)	1320 (0.35)	T	1044 (0.55)	848 (0.45)		
Controls	n = 1898	800 (0.42)	872 (0.46)	226 (0.12)	2472 (0.65)	1324 (0.35)	T	1026 (0.54)	872 (0.46)	.47	
rs10372											
Affected	n = 1902	10 (0.01)	244 (0.13)	1648 (0.87)	264 (0.07)	3540 (0.93)	G	1658 (0.87)	244 (0.13)		
Controls	n = 1904	6 (0.00)	244 (0.13)	1654 (0.87)	256 (0.07)	3552 (0.93)	G	1660 (0.87)	244 (0.13)	.96	
rs3788304											
Affected	n = 1907	1056 (0.55)	720 (0.38)	131 (0.07)	2832 (0.74)	982 (0.26)	G	1187 (0.62)	720 (0.38)		
Controls	n = 1906	1058 (0.56)	720 (0.38)	128 (0.07)	2836 (0.74)	976 (0.26)	G	1186 (0.62)	720 (0.38)	.97	
rs11704083											
Affected	n = 1909	660 (0.35)	915 (0.48)	334 (0.17)	2235 (0.59)	1583 (0.41)	G	994 (0.52)	915 (0.48)		
Controls	n = 1897	646 (0.34)	931 (0.49)	320 (0.17)	2223 (0.59)	1571 (0.41)	G	966 (0.51)	931 (0.49)	.50	

Table 2. Correlation Between Genotype and *GNBIL* Gene Expression in Brain

SNP	Genotype	n	Expression	Genotype	n	Expression	Genotype	n	Expression	P value
rs5746832	AA	19	0.82	AG	16	0.63	GG	21	0.56	.014
Australian	AA	8	0.90	AG	7	0.75	GG	4	0.84	.660
Japanese	AA	11	0.77	AG	9	0.54	GG	17	0.50	.028
rs5746834	GG	46	0.68	GT	11	0.52	TT	2	0.71	.391
rs2269726	TT	22	0.58	TC	20	0.72	CC	15	0.72	.224
rs748806	TT	15	0.84	TC	15	0.55	CC	32	0.63	.105
rs29807124	CC	47	0.68	CT	7	0.85	TT	3	0.29	.063
rs5993835	AA	53	0.61	AG	6	0.62	GG	0	NA	.794
rs 13057609	AA	0	NA	AG	7	0.57	GG	54	0.67	.479
rs4819523	GG	14	0.66	GC	26	0.61	CC	19	0.72	.601
rs2073765	CC	4	0.89	CT	17	0.48	TT	38	0.70	.520
rs7286924	AA	33	0.64	AT	21	0.77	TT	9	0.49	.112
rs10372	AA	0	NA	AG	8	0.67	GG	52	0.52	.261
rs3788304	CC	37	0.65	CG	21	0.64	GG	5	0.73	.731
rs11704083	AA	22	0.75	AG	23	0.56	GG	17	0.67	.412

due to cis-acting differences by genetic polymorphisms in this locus or not in this study.

The present study showed that reduced expression of *GNBIL* may be involved in the pathophysiology of schizophrenia; however, it does not exclude the possibility that other genes in the 22q11DS region contribute to the susceptibility to schizophrenia. The array used in the present study did not examine all isoforms of the genes in

the 22q11DS region. In addition, the reliability of weakly expressed sequences in the array screening is not sufficient. Therefore, we reexamined expression levels of the genes, which reliable data (greater than 0.96 confidence) was produced by the array in no subjects, by real-time PCR method. The study is also limited by the areas and ages of the brains examined. We examined only adult postmortem prefrontal cortex. Differential gene expression in other brain regions or during other developmental stages may also influence the susceptibility to schizophrenia.

The consortium data of the Stanley Medical Research Institute showed no significant differences ( $P > .05$ ) in the following gene expression levels in postmortem prefrontal cortex between patients with schizophrenia and controls: *DGCR6*, *PRODH*, *DGCR2*, *STK22B*, *DGCR14*, *CLTCL1*, *CLTCL1*, *HIRA*, *UFD1L*, *CDC45L*, *CLDN5*, *TBX1*, *FLJ21125*, *TXNRD2*, *COMT*, *ARVCF*, *DKFZp761P1121*, *DGCR8*, *HTF9C*, *RANBP1*, and *ZDHHC8*. The expression of *RTN4R* might be potentially reduced ( $P = .02$ ). No data were available for *GSCL*, *MRPL40*, *SEPT5*, *GPIBB*, and *GNBIL* (<http://www.stanleyresearch.org/brain/menu.asp>).

A trans-acting effect on expression of the disease gene may also be expected to modulate disease susceptibility. Large-scale studies in humans have indicated that a significant proportion of the heritable variance in gene expression is attributable to trans-acting polymorphism.<sup>33,34</sup> As one of the examples, recent study reported that microRNAs regulate gene expression posttranscriptionally.<sup>35</sup> Even for schizophrenia, Bray et al.<sup>36</sup> indicated that the reduction in *DTNBP1* expression in schizophrenia is likely to result in part from trans-acting risk factors. Such

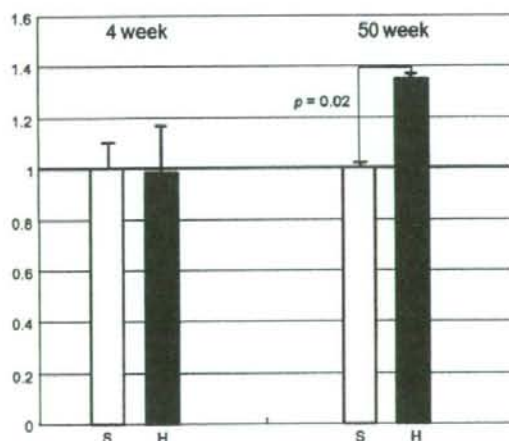


Fig. 3. Effect of haloperidol treatment on *Gnb1* expression. Relative expression of the *Gnb1* gene in mouse prefrontal cortex in saline treated (S) or haloperidol treated (H) mice during 4 or 50 weeks. The vertical scale shows relative *Gnb1* expression compared with that in saline-treated mice, with bars for  $\pm 1$  SD calculated in each group, respectively.

trans-acting factors that regulate *GNBIL* gene expression, however, have not been identified.

In conclusion, the present study further supports the role of *GNBIL* in the pathophysiology of schizophrenia.

#### Supplementary Material

Supplementary tables are available at <http://schizophreniabulletin.oxfordjournals.org/>.

#### Funding

Grant-in-Aid for Scientific Research on Priority Areas; Research on Pathomechanisms of Brain Disorders from the Ministry of Education, Culture, Sports, Science and Technology of Japan (20390098 and 20023006); Japan Science and Technology.

#### Acknowledgments

Australian human brain tissues were received from the NSW Tissue Resource Centre, which is supported by The University of Sydney, Neuroscience Institute of Schizophrenia and Allied Disorders National Institute of Alcohol Abuse and Alcoholism and NSW Department of Health.

#### References

- Bassett AS, Chow EW. 22q11 deletion syndrome: a genetic subtype of schizophrenia. *Biol Psychiatry*. 1999;46:882-891.
- Karayorgou M, Gogos JA. The molecular genetics of the 22q11-associated schizophrenia. *Brain Res Mol Brain Res*. 2004;132:95-104.
- Funke B, Edelmann L, McCain N, et al. Der(22) syndrome and velo-cardio-facial syndrome/DiGeorge syndrome share a 1.5-Mb region of overlap on chromosome 22q11. *Am J Hum Genet*. 1999;64:747-758.
- Shaikh TH, Kurahashi H, Saitta SC, et al. Chromosome 22-specific low copy repeats and the 22q11.2 deletion syndrome: genomic organization and deletion endpoint analysis. *Hum Mol Genet*. 2000;9:489-501.
- Yagi H, Furutani Y, Hamada H, et al. Role of *TBX1* in human del22q11.2 syndrome. *Lancet*. 2003;362:1366-1373.
- Stoller JZ, Epstein JA. Identification of a novel nuclear localization signal in *Tbx1* that is deleted in DiGeorge syndrome patients harboring the 1223delC mutation. *Hum Mol Genet*. 2005;14:885-892.
- Merscher S, Funke B, Epstein JA, et al. *TBX1* is responsible for cardiovascular defects in velo-cardio-facial/DiGeorge syndrome. *Cell*. 2001;104:619-629.
- Lindsay EA, Vitelli F, Su H, et al. *Tbx1* haploinsufficiency in the DiGeorge syndrome region causes aortic arch defects in mice. *Nature*. 2001;410:97-101.
- Paylor R, Glaser B, Mupo A, et al. *Tbx1* haploinsufficiency is linked to behavioral disorders in mice and humans: implications for 22q11 deletion syndrome. *Proc Natl Acad Sci U S A*. 2006;103:7729-7734.
- Takase K, Ohtsuki T, Migita O, et al. Association of *ZNF74* gene genotypes with age-at-onset of schizophrenia. *Schizophr Res*. 2001;52:161-165.
- Shifman S, Levit A, Chen ML, et al. A complete genetic association scan of the 22q11 deletion region and functional evidence reveal an association between *DGCR2* and schizophrenia. *Hum Genet*. 2006;120:160-170.
- Wang H, Duan S, Du J, et al. Transmission disequilibrium test provides evidence of association between promoter polymorphisms in 22q11 gene *DGCR14* and schizophrenia. *J Neural Transm*. 2006;113:1551-1561.
- Jacquet H, Raux G, Thibaut F, et al. *PRODH* mutations and hyperprolinemia in a subset of schizophrenic patients. *Hum Mol Genet*. 2002;11:2243-2249.
- Mukai J, Liu H, Burt RA, et al. Evidence that the gene encoding *ZDHHC8* contributes to the risk of schizophrenia. *Nat Genet*. 2004;36:725-731.
- Bray NJ, Buckland PR, Williams NM, et al. A haplotype implicated in schizophrenia susceptibility is associated with reduced *COMT* expression in human brain. *Am J Hum Genet*. 2003;73:152-161.
- Dempster EL, Mill J, Craig IW, Collier DA. The quantification of *COMT* mRNA in post mortem cerebellum tissue: diagnosis, genotype, methylation and expression. *BMC Med Genet*. 2006;7:10.
- Nicodemus KK, Kolachana BS, Vakkalanka R, et al. Evidence for statistical epistasis between catechol-O-methyltransferase (*COMT*) and polymorphisms in *RGS4*, *G72* (*DAOA*), *GRM3*, and *DISC1*: influence on risk of schizophrenia. *Hum Genet*. 2007;120:889-906.
- Shifman S, Bronstein M, Sternfeld M, et al. A highly significant association between a *COMT* haplotype and schizophrenia. *Am J Hum Genet*. 2002;71:1296-1302.
- Sun ZY, Wei J, Xie L, et al. The *CLDN5* locus may be involved in the vulnerability to schizophrenia. *Eur Psychiatry*. 2004;19:354-357.
- Ye L, Sun Z, Xie L, et al. Further study of a genetic association between the *CLDN5* locus and schizophrenia. *Schizophr Res*. 2005;75:139-141.
- Faul T, Gawlik M, Bauer M, et al. *ZDHHC8* as a candidate gene for schizophrenia: analysis of a putative functional intronic marker in case-control and family-based association studies. *BMC Psychiatry*. 2005;5:35.
- Glaser B, Moskvina V, Kirov G, et al. Analysis of *ProDH*, *COMT* and *ZDHHC8* risk variants does not support individual or interactive effects on schizophrenia susceptibility. *Schizophr Res*. 2006;87:21-27.
- Li D, He L. Association study of the G-protein signaling 4 (*RGS4*) and proline dehydrogenase (*PRODH*) genes with schizophrenia: a meta-analysis. *Eur J Hum Genet*. 2006;14:1130-1135.
- Munafò MR, Bowes L, Clark TG, Flint J. Lack of association of the *COMT* (Val158/108 Met) gene and schizophrenia: a meta-analysis of case-control studies. *Mol Psychiatry*. 2005;10:765-770.
- Hiroi N, Zhu H, Lee M, et al. A 200-kb region of human chromosome 22q11.2 confers antipsychotic-responsive behavioral abnormalities in mice. *Proc Natl Acad Sci U S A*. 2005;102:19132-19137.
- Williams NM, Glaser B, Norton N, et al. Strong evidence that *GNBIL* is associated with schizophrenia. *Hum Mol Genet*. 2008;17:555-566.
- Centonze D, Usiello A, Costa C, et al. Chronic haloperidol promotes corticostriatal long-term potentiation by targeting dopamine D2L receptors. *J Neurosci*. 2004;24:8214-8222.

28. Leite JV, Guimaraes FS, Moreira FA. Aripiprazole, an atypical antipsychotic, prevents the motor hyperactivity induced by psychotomimetics and psychostimulants in mice. *Eur J Pharmacol.* 2008;578:222–227.
29. Duncan GE, Moy SS, Lieberman JA, Koller BH. Effects of haloperidol, clozapine, and quetiapine on sensorimotor gating in a genetic model of reduced NMDA receptor function. *Psychopharmacology (Berl).* 2006;184:190–200.
30. Narayan S, Kass KE, Thomas EA. Chronic haloperidol treatment results in a decrease in the expression of myelin/oligodendrocyte-related genes in the mouse brain. *J Neurosci Res.* 2007;85:757–765.
31. Nagai T, Murai R, Matsui K, et al. Aripiprazole ameliorates phencyclidine-induced impairment of recognition memory through dopamine D(1) and serotonin 5-HT (1A) receptors. *Psychopharmacology (Berl).* 2008 First published in August 6, 2008, DOI:10.1007/s00213-008-1240-6.
32. Funke B, Epstein JA, Kochilas LK, et al. Mice overexpressing genes from the 22q11 region deleted in velo-cardio-facial syndrome/DiGeorge syndrome have middle and inner ear defects. *Hum Mol Genet.* 2001;10:2549–2556.
33. Monks SA, Leonardson A, Zhu H, et al. Genetic inheritance of gene expression in human cell lines. *Am J Hum Genet.* 2004;75:1094–1105.
34. Morley M, Molony CM, Weber TM, et al. Genetic analysis of genome-wide variation in human gene expression. *Nature.* 2004;430:743–747.
35. Pitto L, Ripoli A, Cremisi F, Simili M, Rainaldi G. Micro-RNA(interference) networks are embedded in the gene regulatory networks. *Cell Cycle.* 2008;7(16):2458–2461.
36. Bray NJ, Holmans PA, van den Bree MB, et al. Cis- and trans-loci influence expression of the schizophrenia susceptibility gene DTNBP1. *Hum Mol Genet.* 2008;17:1169–1174.

Please cite this article in press as: Namba H, et al., Epidermal growth factor administered in the periphery influences excitatory synaptic inputs onto midbrain dopaminergic neurons in postnatal mice, *Neuroscience* (2008), doi: 10.1016/j.neuroscience.2008.10.057

*Neuroscience* xx (2008) xxx

## EPIDERMAL GROWTH FACTOR ADMINISTERED IN THE PERIPHERY INFLUENCES EXCITATORY SYNAPTIC INPUTS ONTO MIDBRAIN DOPAMINERGIC NEURONS IN POSTNATAL MICE

H. NAMBA,\* Y. ZHENG,\* Y. ABE\* AND H. NAWA<sup>a,b,\*</sup>

<sup>a</sup>Division of Molecular Neurobiology, Brain Research Institute, Niigata University, 1-757 Asahimachi, Chuo-ku, Niigata 951-8585, Japan

<sup>b</sup>Center for Transdisciplinary Research, Niigata University, Niigata 950-2181, Japan

**Abstract**—Epidermal growth factor (EGF) has a neurotrophic activity on developing midbrain dopaminergic neurons. We investigated developmental effects of peripheral EGF administration on dopaminergic neurons in midbrain slice preparations containing ventral tegmental area (VTA). Subcutaneous EGF administration to mouse neonates triggered phosphorylation of EGF receptors (ErbB1 and ErbB2) in the midbrain region, suggesting its penetration through the blood–brain barrier. We repeated EGF administration in postnatal mice and examined synaptic transmission in the VTA with electrophysiological recordings. Subchronic EGF treatment increased the amplitude of field excitatory postsynaptic potentials evoked by stimulation of the anterior VTA. To analyze the EGF effect at a single cell level, dopaminergic neurons were identified by their characteristic hyperpolarizing activated currents in whole cell recording. In these dopaminergic neurons, EGF effects the amplitude of spontaneous miniature excitatory postsynaptic currents (mEPSCs) without affecting their frequency. In agreement, EGF also enhanced the AMPA/NMDA ratio of evoked EPSCs in the dopaminergic neurons. In contrast, EGF effects on mEPSCs of neighboring neurons not exhibiting hyperpolarizing activated currents were modest or insignificant. Thus, these results suggest that circulating EGF substantially influences the physiological properties of developing midbrain dopaminergic neurons in perinatal and postnatal mice. © 2008 IBRO. Published by Elsevier Ltd. All rights reserved.

**Key words:** neurotrophic factor, dopamine, ventral tegmental area, AMPA, ErbB1.

Epidermal growth factor (EGF) and EGF homologues have the neurotrophic activity that promotes survival and neurite

\*Correspondence to: H. Nawa, Division of Molecular Neurobiology, Brain Research Institute, Niigata University, 1-757 Asahimachi, Chuo-ku, Niigata 951-8585, Japan.

E-mail address: hnawa@bri.niigata-u.ac.jp (H. Nawa).

Abbreviations: ACSF, artificial cerebrospinal fluid; ANOVA, analysis of variance; AP, alkaline phosphatase; CNQX, 6-cyano-7-nitroquinoxaline-2,3-dione; DiG, digoxigenin; EGF, epidermal growth factor; EPSC, excitatory postsynaptic current; EPSP, excitatory postsynaptic potential; ErbB1, epidermal growth factor receptor; fr, fasciculus retroflexus; GFAP, glial fibrillary acidic protein;  $I_h$ , hyperpolarizing activated current; K-S, Kolmogorov-Smirnov; mEPSC, miniature excitatory postsynaptic currents; MT, medial terminal nucleus of the accessory optic tract; NaPB, sodium phosphate buffer; NSE, neuron-specific enolase; P, postnatal day; SDS, sodium dodecyl sulfate; SNc, substantia nigra compacta; TBS, Tris-buffered saline; VTA, ventral tegmental area.

0306-4522/08 © 2008 IBRO. Published by Elsevier Ltd. All rights reserved. doi:10.1016/j.neuroscience.2008.10.057

elongation of midbrain dopaminergic neurons (Casper et al., 1991; Casper and Blum, 1995; Alexi and Hefti, 1993; Ferrari et al., 1991; Iwakura et al., 2005; Pezzoli et al., 1991). Repeated injection of EGF into rat neonates or subchronic infusion into the striatum of adult rats increases dopamine metabolism and/or tyrosine hydroxylase activity *in vivo* (Futamura et al., 2003; Tohmi et al., 2005; Mizuno et al., 2007). Epidermal growth factor receptor (ErbB1) mRNA is widely expressed in the CNS including midbrain regions (Kornblum et al., 1997; Fox and Kornblum, 2005). Previous *in situ* hybridization studies suggest that the rat ventral tegmental area (VTA) and substantia nigra compacta (SNc) express ErbB1 mRNA (Seroogy et al., 1994; Kornblum et al., 1997). In addition, a null mutation for an ErbB1 ligand, transforming growth factor  $\alpha$ , reduces the number of dopaminergic neurons in the SNc (Blum, 1998). Thus, EGF signaling in the midbrain is implicated in regulation of dopaminergic function or development.

EGF is synthesized in many peripheral organs, including the kidney, liver and pituitary gland; it is released into the bloodstream and crosses the blood–brain barrier (Kastin et al., 1999; Pan and Kastin, 1999). Transforming growth factor  $\alpha$  and heparin-binding EGF-like growth factor are, however, produced endogenously in the CNS and contribute to the activation of ErbB1 as well (Birecree et al., 1991; Schaudies et al., 1989; Lazar and Blum, 1992; Piao et al., 2005). Although EGF mRNA and protein are also expressed endogenously in restricted regions of the brain, their levels are relatively low in comparison with EGF concentrations in blood (Futamura et al., 2002). Concentrations of EGF in human blood are relatively high with a picomolar range and altered in several brain diseases of developmental origin (Futamura et al., 2002; Ikeda et al., 2008). Presumably, circulating EGF could have strong impact on development of the CNS, especially in the fetus where the blood–brain barrier is not fully established (see review: Plata-Salaman, 1991). In this context, it is unclear how influential circulating EGF is in brain development or function. In particular, evidence for the neurotrophic effects of peripheral EGF on dopaminergic development is very limited.

Here we assessed subchronic effects of EGF administered to the periphery on postnatal dopaminergic neurons in the VTA, focusing on the excitatory synapses formed on these neurons. Strength of excitatory inputs to midbrain dopaminergic neurons is regulated in a plastic manner (White, 1996) and the plasticity is often implicated in the regulation of dopaminergic function (Giorgetti et al., 2001). Thus, we analyzed presynaptic and postsynaptic properties of the excitatory inputs to dopaminergic neurons,

employing field potential recordings and slice patch-clamp recordings. Protein levels of ionotropic glutamate receptor subunits were measured by immunoblotting and compared with the electrophysiological results. Physiological and pathologic implication of circulating EGF was discussed.

## EXPERIMENTAL PROCEDURES

### Animal protocols

Neonatal mice at postnatal day 2 (P2) or pregnant mice at 15 gestation days of C57BL/6 strain, were purchased from SLC (Shizuoka, Japan). Recombinant human EGF (0.875  $\mu\text{g/g}$  body weight, Higeta Shoyu, Chiba, Japan) was administered s.c. to half of the pups in newborn litters daily for 2 weeks (P2–15) (Tohmi et al., 2005; Nagano et al., 2007). The dose of EGF does not impair physical growth of mice (Tohmi et al., 2005). Control littermates received a saline injection. All postnatal mice were housed with a dam until weaning (a litter per cage; 13.6L $\times$ 20.8W $\times$ 11.5H cm). All mice were housed on a 12-h light/dark cycle with free access to food and water. All animal experiments were authorized by the Animal Use and Care Committee of Niigata University and were carried out in accordance with the National Institutes of Health guidelines for care and use of laboratory animals. All efforts were made to minimize the number of animals used and their suffering.

### Biotinylation of human EGF and injection

To visualize permeation of EGF through the blood–brain barrier, human recombinant EGF was biotinylated with the following procedure. EGF (35  $\mu\text{g}/\mu\text{l}$ , Higeta Shoyu) was incubated with EZ-Link sulfo-NHS-LC-biotin (No. 21335, Pierce, Rockland, IL, USA) at a molar ratio to EGF of 50:1 overnight at 4 °C. The reaction mixture was dialyzed for two overnight sessions to remove an uncoupled biotinylation reagent (Slide-A-Lyzer 3.5K, Pierce No. 66330). Biotinylated EGF was s.c. injected (0.8  $\mu\text{g/g}$  body weight) to neonatal mice at P2 as described above.

### Fixation and tissue preparation

Mice were anesthetized with hypothermia on ice and transcardially perfused with 4% paraformaldehyde in 0.1 M sodium phosphate buffer (NaPB), pH 7.4. Brains were post-fixed overnight with the same paraformaldehyde solution. Then, the tissue was immersed in 30% sucrose in 0.1 M NaPB and embedded in OCT compound (Sakura Finetek, Torrance, CA, USA). Coronal or horizontal sections (12–14  $\mu\text{m}$  thick) were prepared for *in situ* hybridization and immunohistochemistry using the cryostat (CM1510, Leica, Nussloch, Germany).

### In situ hybridization

cRNA probes were synthesized as follows: A cDNA fragment for ErbB1 mRNA was synthesized from mouse brain RNA using Platinum<sup>®</sup> Pfx DNA polymerase (Invitrogen, Carlsbad, CA, USA) and oligoDNA primers. The primers carried DNA sequences matching mouse ErbB1 gene (GenBank: NM\_207655) as well as T7 or SP6 promoter sequences (SP6: cgatttaggtgacactatagatagtgactctctggctgcaaaagtt; T7: gtaatacactcactataggccctccgaggagcacaagaattg; 850 bp). Digoxigenin (DIG)-labeled sense and anti-sense cRNA probes were made by *in vitro* transcription with SP6 and T7 RNA polymerases, respectively (Roche Diagnostics, Indianapolis, IN, USA) (Young et al., 1991).

*In situ* hybridization was carried out as previously described (Liang et al., 2000; Watakabe et al., 2006). In brief, sections (14  $\mu\text{m}$  thick) were treated with proteinase K (0.2  $\mu\text{g}/\text{ml}$ ). After acetylation, sections were hybridized with 1  $\mu\text{g}/\text{ml}$  DIG-labeled cRNA probes at 60 °C for 6 h. Sections were washed with 2 $\times$  SSC (0.3 M NaCl, 0.03 M sodium citrate, pH 7.0)/50% formamide/0.1%

N-lauroylsarcosine for 20 min at 60 °C and then treated with 20  $\mu\text{g}/\text{ml}$  RNase A (Sigma-Aldrich, St Louis, MO, USA) for 30 min at 37 °C. To detect hybridization signals, sections were incubated with alkaline phosphatase (AP)-conjugated sheep anti-DIG antibody (1:1000, Roche Diagnostics) for 4 h at room temperature, and then AP activity was visualized with nitro blue tetrazolium chloride (NBT) and 5-bromo-4-chloro-3-indolyl phosphate, toluene salt (BCIP) as substrates (Roche Diagnostics).

### Immunohistochemistry

For immunostaining, sections (12  $\mu\text{m}$  thick) were incubated with 5% bovine serum albumin and 0.3% Triton X-100 in Tris-buffered saline (TBS; 0.1 M Tris-HCl pH 7.4, 150 mM NaCl) for 1 h and then treated with an anti-tyrosine hydroxylase antibody (1/1000, rabbit polyclonal, Chemicon or 1/1000 mouse monoclonal) (Hatanaka and Arimatsu, 1984) overnight. After rinsing with TBS, sections were incubated with biotin-labeled rabbit or mouse secondary antibodies (1/200, Vector Laboratories, Burlingame, CA, USA), followed by incubation with Vectastain ABC elite kit (1:100). Immunoreactivity was visualized with 3,3'-diaminobenzidine (DAB).

### Electrophysiology

Mice (P16–18) were anesthetized with halothane and decapitated. Brains were removed and placed in a cold artificial cerebrospinal fluid (ACSF) solution containing the following (in mM): 195 sucrose, 1  $\text{NaH}_2\text{PO}_4$ , 2.5 KCl, 5  $\text{MgSO}_4$ , 1.0  $\text{CaCl}_2$ , 26.2  $\text{NaHCO}_3$ , 11  $\text{D-glucose}$ , 1 ascorbic acid, pH 7.4, and saturated with 95%  $\text{O}_2$  and 5%  $\text{CO}_2$ . For field recordings, horizontal slices (thickness: 500  $\mu\text{m}$ ) containing the VTA were prepared with a microslicer (DTK-2000 or Pro7, Dosaka, Kyoto, Japan) and dissected at the midline according to Zheng et al. (2006). Slices were placed in an incubation chamber for at least 1 h at room temperature. The chamber was filled with an ACSF solution containing the following (in mM): 119 NaCl, 1.0  $\text{NaH}_2\text{PO}_4$ , 2.5 KCl, 1.3  $\text{MgSO}_4$ , 2.5  $\text{CaCl}_2$ , 26.2  $\text{NaHCO}_3$ , 11  $\text{D-glucose}$ , and 1 ascorbic acid.

Electrophysiological experiments were all performed at room temperature (24–26 °C). Slices were placed in a recording chamber continuously perfused with normal ascorbic acid-free ACSF at  $\sim$ 4.0 ml/min. The VTA was identified as the region lateral to the fasciculus retroflexus (fr) and medial to the medial terminal nucleus of the accessory optic tract (MT) (Johnson and North, 1992; Zheng et al., 2006). Field recording procedures were modified in accordance with our previous experiments with slices of rat brain (Zheng et al., 2006). A glass microelectrode filled with ACSF (5–8 M $\Omega$ ) was placed between fr and MT. Field potentials were evoked by electrical stimuli (50  $\mu\text{s}$  duration, 0.05 Hz) from the micro-concentric electrode (tip diameter; 25  $\mu\text{m}$ , MCE-100, David Kopf Instruments, Tujunga, CA, USA), which was located at the anterolateral position of the recording electrode. The anterior region of the VTA contains glutamatergic fibers possibly originated from prefrontal cortex, hypothalamus, and other brain regions (Geisler et al., 2007). Field potentials were recorded with 0.1 mA increments of stimulus intensity (0.12–0.62 mA) in the presence of 20  $\mu\text{M}$  bicuculline. The amplitude of fiber volley component (N1) was calculated with the program for population spike measurement in Axograph 3.5 (Axon Instruments) to compensate for the stimulation artifacts. To measure the amplitude of the CNQX-sensitive component (N2), field excitatory postsynaptic potential (EPSP), five responses were averaged in each stimulus intensity and the peak difference in amplitude before and after CNQX application was calculated with Clampfit 6 (Axon Instruments, Foster City, CA, USA) (Zheng et al., 2006).

For whole cell recordings, horizontal slices (thickness: 250  $\mu\text{m}$ ) were prepared. Individual cells in the medial region of MT were visualized with an upright phase microscope. Whole-cell patch-clamp recordings were made with an Axopatch 200B (Axon Instruments). Dopaminergic neurons were identified by their char-

**Table 1.** Passive properties of midbrain dopaminergic and non-dopaminergic neurons in EGF-treated mice

	Vm (mV)	Rm (MΩ)	Cm (pF)	Rs (MΩ)	I <sub>n</sub> (pA)
DA neuron					
cont (n=13)	-56.8±1.2	410±53	79.5±3.9	16.0±0.7	139±35
EGF (n=13)	-56.9±1.3	375±53	96.9±8.1	14.6±1.0	155±47
Non-DA neuron					
cont (n=9)	-55.4±2.0	698±185	59.5±4.8	21.9±1.4	15±4
EGF (n=9)	-59.6±1.7	701±143	60.0±8.0	21.4±1.4	20±6

Input resistance and series resistance were determined by measuring the current response to a negative 5 mV pulse from a holding potential. Cell capacitance measurements were made by integration of capacitive transients. I<sub>n</sub> was measured by 900 ms of hyperpolarizing voltage steps of -70 mV from holding potential at -69 mV. Cells displaying >40 pA of I<sub>n</sub> currents were classified to putative dopaminergic (DA) neurons. We confirmed that more than 70% of the cells in this criteria carried tyrosine hydroxylase immunoreactivity (data not shown). Abbreviations: Vm, membrane potential; Rm, input resistance; Cm, membrane capacitance; Rs, series resistance.

acteristic hyperpolarizing activated current (I<sub>n</sub>) (more than 40 pA; see Table 1) (Johnson and North, 1992). For miniature excitatory postsynaptic current (mEPSC) analysis, a pipette (3–5 MΩ) was filled with an internal solution containing (in mM), 122.5 KMeSO<sub>3</sub>, 7.5 KCl, 10 Hepes, 0.2 EGTA, 5 biocytin-Cl, and 4 Mg-ATP and sucrose to adjust the osmolarity to 290 mOsm (pH 7.4). Membrane and holding potentials were compensated with the liquid junction potential (-9 mV). All data were filtered at 2 kHz and digitized at a sampling rate of 10 kHz. Data were acquired using Axoclamp7 (Axon Instruments). Spontaneous mEPSCs were recorded in the presence of 1 μM tetrodotoxin and 10 μM bicuculline. No compensation for whole-cell capacitance or series resistance was made. Series resistance was determined by measuring a current response to a negative 5 mV pulse from the holding potential. Recording with a series resistance of more than 30 MΩ or cases in which the series resistance changed by more than 10% were excluded. Miniature events were detected with a threshold level for detection of 6 pA with the Mini Analysis Program (Jaeger Software, Leonia, NJ, USA). One hundred twenty events were pooled and analyzed in each cell.

To assess the contribution of AMPA receptor-mediated and NMDA-receptor-mediated components to evoked excitatory postsynaptic currents (EPSCs), whole cell recordings were performed with a patch pipette (3–5 MΩ) containing (in mM) 117 CsMeSO<sub>3</sub>, 2.8 NaCl, 20 Hepes, 0.4 EGTA, 5 TEA-Cl, 2.5 Mg-ATP, and 5 QX314Cl and sucrose to adjust the osmolarity to 290 mOsm (pH 7.4) (Ungless et al., 2001). Holding potentials were compensated with the liquid junction potential (-6 mV). Synaptic currents were evoked by constant electrical stimuli (0.05–0.2 mA, 50 μs duration, 0.067 Hz) with a micro-concentric bipolar electrode (tip-diameter: 25 μm; MCE-100, David Kopf Instruments), placed 100–300 μm antero-lateral to the recording position. AMPA currents were recorded at holding potential of -66 mV in the presence of 10 μM bicuculline. NMDA currents were recorded in the presence of 10 μM 6-cyano-7-nitroquinoline-2,3-dione (CNQX) and 10 μM bicuculline at holding potential of 34 mV. Ten traces of synaptic events in each cell were averaged with Clampfit 6 (Axon Instruments) and the peak amplitude from the reflection point was measured. The ratio of these currents was calculated as the AMPA/NMDA ratio.

### Immunoblotting

For immunoblotting analysis, we dissected the VTA region with two different procedures. In the first procedure, one 800-μm thick horizontal slice including VTA was prepared with a micro-slicer and cold high sucrose ACSF (see above). The VTA region, located medially between MT, was dissected with a surgical blade under a stereoscopic microscope with coordinates from the mouse brain atlas (see Fig. 5A) (Paxinos and Franklin, 2004; see also Zheng et al., 2006). Tissues obtained from two animals were pooled. In the second procedure, a coronal slice (1 mm of

thickness) was dissected from ventral side with a pair of razor blades and the medial region between MT was dissected. Tissues were homogenized with Laemmli sample buffer (2% sodium dodecyl sulfate (SDS), 62.5 mM Tris pH 6.8). Consistent results were obtained with samples prepared with either procedure.

To detect phosphorylation of ErbB1 and ErbB2, whole brain was dissected 45 min after s.c. administration of EGF (Nagano et al., 2007; Tohmi et al., 2005). A coronal slice of the midbrain (1 mm of thickness) was dissected from the ventral side with a pair of razor blades. Ventral midbrain tissue was quickly homogenized in a 2% SDS buffer containing phosphatase inhibitors (2 mM NaVO<sub>3</sub>, 10 mM NaF) and a protease inhibitor cocktail (Complete Mini, Roche, Mannheim, Germany) (see also Fig. 1A). After centrifugation, supernatants were denatured at 95 °C in the presence of 5% 2-mercaptoethanol and 10% glycerol. Protein concentrations were measured with the Micro BCA kit (Pierce) using bovine serum albumin as a standard. Protein (5–30 μg/lane) was separated by SDS-polyacrylamide gel electrophoresis and transferred to a polyvinylidene difluoride membrane by electrophoresis. Primary antibodies were diluted (see below) and incubated with the membrane at 4 °C overnight. Immunoreactivity was detected with goat anti-mouse, anti-rabbit immunoglobulin, or rabbit anti-goat immunoglobulin conjugated to peroxidase (1:10,000; Vector Laboratories), and visualized with a chemiluminescence reaction (ECL kit, Amersham Biosciences, Tokyo, Japan). Primary antibodies were used at the following dilutions: anti-phospho-ErbB1 (Tyr1173; 1/500, sc-12351), anti-ErbB1 (1/500; sc-03), anti-ErbB2 (1/500; Neu C-18, sc-284) (all from Santa Cruz, Santa Cruz, CA, USA), and anti-phospho-ErbB2 (Tyr1248) (1/2000; #06-229, Upstate, Millipore, Billerica, MA, USA) (Kim et al., 1999). Anti-GluR1, anti-GluR2/3, anti-NR1, anti-NR2A and anti-NR2B antibodies were purchased from Chemicon International (Temecula, CA, USA) and GluR4 (rabbit) was from Upstate. Anti-glial fibrillary acidic protein (GFAP) antibody was from DAKO (Glostrup, Denmark) and anti-neuron-specific enolase (NSE) antibody from Polysciences Inc. (Warrington, PA, USA). Rabbit anti-synapsin I and mouse anti-synaptophysin antibodies were obtained from Dr. E. Miyamoto and Dr. M Takahashi, respectively (Obata et al., 1986; Fukunaga et al., 2002).

### Statistical analysis

Results are presented as the means ± S.E.M. Electrophysiological data were subjected to parametric analysis by analysis of variance (ANOVA) or univariate analysis with Student's *t*-test. Data of mEPSCs were also subjected to the non-parametric analysis, Kolmogorov-Smirnov (*K-S*) test to avoid type 2 statistical errors. To quantify immunoreactivity on blots, the densitometry of bands (arbitrary units) was performed and subjected to *t*-test. A *P* value of less than 0.05 was considered statistically significant. Statistical analysis was performed using the SPSS software (version 11.5; SPSS Japan Inc., Tokyo, Japan).

Please cite this article in press as: Namba H, et al., Epidermal growth factor administered in the periphery influences excitatory synaptic inputs onto midbrain dopaminergic neurons in postnatal mice, *Neuroscience* (2008), doi: 10.1016/j.neuroscience.2008.10.057

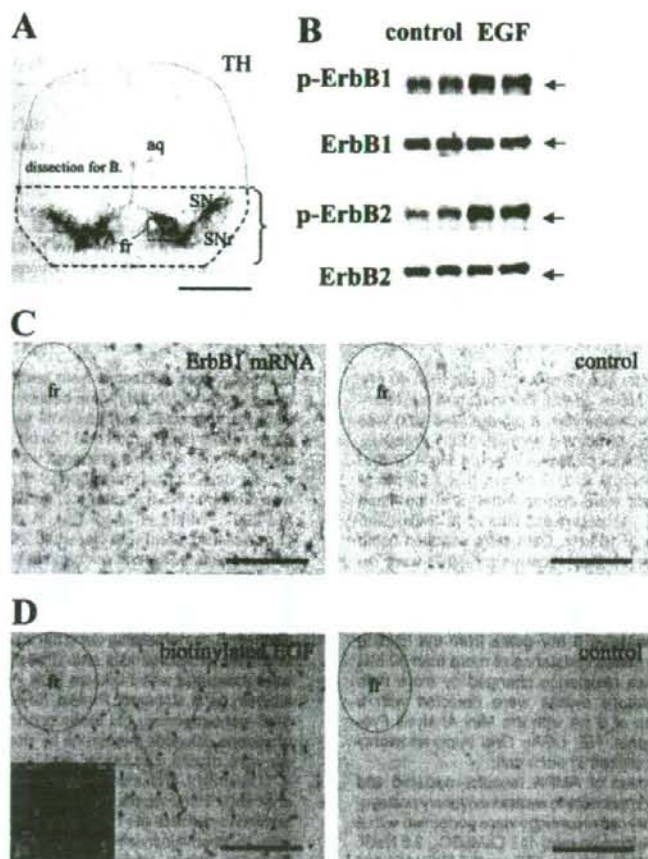


**Fig. 1.** Acute phosphorylation of ErbB1 and ErbB2 in the ventral midbrain following s.c. administration of EGF. EGF (0.875  $\mu\text{g/g}$  body weight) was s.c. injected into neonatal mice at P2. The midbrain region indicated in A was taken 45 min after administration. Protein lysate (30  $\mu\text{g}$ ) was loaded and separated on 7.5% SDS-PAGE gels and transferred to membranes. (A) Typical distributions of tyrosine hydroxylase immunoreactivity of the present slice preparation are displayed; aqueduct (aq), fr, SNc, and substantia nigra reticulata (SNr). (B) Membranes were probed with anti-phospho ErbB1 and anti-ErbB1 antibodies or anti-phospho-ErbB2 and anti-ErbB2 antibodies. No alterations were observed in the total levels of ErbB1 and ErbB2. Arrows indicate the molecular size of 175 kDa. (C) Distributions of ErbB1 mRNA were examined in the midbrain region by *in situ* hybridization with an antisense probe. Control sections were probed with a sense probe for ErbB1 mRNA. Coronal sections containing the VTA were selected with the presence of fr. (D) Biotinylated EGF was similarly injected to mouse neonates. EGF penetration to midbrain through the blood-brain barrier was assessed by the avidin-biotin-complex method. Adjoining serial sections were immunostained with anti-tyrosine hydroxylase antibody as shown in A. The position of a window in A roughly matched that of C and D. The inset in D indicates the accumulation of biotinylated EGF in a cell body. Scale bars = 1 mm (A); 100  $\mu\text{m}$  (C), (D).

## RESULTS

### Peripherally administered EGF penetrated the blood-brain barrier

To estimate the permeability of EGF to the blood-brain barrier, we monitored acute phosphorylation of ErbB1 and its subunit (ErbB2) following s.c. injection of EGF to mouse neonates. Immunoblotting revealed that EGF administration increased the immunoreactivity for phospho-ErbB1 in the ventral midbrain region without changing the levels of total ErbB1 immunoreactivity (Fig. 1A, 1B). The increase in phospho-ErbB1 immunoreactivity

was confirmed by the other immunoblot with the different antibody (data not shown). EGF administration also increased phosphorylation of ErbB2. In agreement, *in situ* hybridization detected ErbB1 mRNA in the midbrain region (Fig. 1C). We attempted to confirm that the phosphorylation of ErbB1 resulted from the penetration of administered EGF through the blood-brain barrier but not secondary release of endogenous EGF. In the place of authentic EGF, biotinylated EGF was s.c. injected to mouse neonates and localization of biotin signals was examined using the avidin-peroxidase complex. Significant levels of biotin signals were detected in the cell



bodies in the midbrain region (Fig. 1D). In contrast, the signals in a saline-injected control animal were modest or negligible. These results suggest that EGF circulating in blood can reach midbrain neurons of neonatal mice and influence their function and development.

#### EGF treatment increased amplitudes of field EPSP in the VTA

We assessed gross physiological influences of the EGF penetration to the VTA with field potential recording (Zheng et al., 2006; Nugent et al., 2008). In the previous study, we found that more than half of the response to stimulation detected by field recordings reflects synaptic inputs onto dopaminergic neurons (Zheng et al., 2006). The field potentials recorded in the presence of 20  $\mu$ M bicuculline exhibited two negative components, an N1 action potential component and an N2 synaptic component that was sensitive to CNQX (Fig. 2). The amplitude of N1 increased linearly with stimulus intensity. The N1 amplitude was not altered by EGF administration, however ( $P=0.47$ ; two-way repeated measures ANOVA). In contrast, postnatal EGF administration significantly increased the amplitude of CNQX-sensitive N2 synaptic component ( $P=0.042$ ). The peak latencies of N1 and N2 were not statistically different between groups at the stimulus intensity of 0.62 mA ([N1] control:  $2.0 \pm 0.1$  ms; EGF:  $2.0 \pm 0.1$  ms,  $P=0.63$ ; [N2] control:  $5.8 \pm 0.4$  ms; EGF:  $5.1 \pm 0.2$  ms,  $P=0.16$ ). Thus, EGF administration enhanced the AMPA receptor-mediated component of synaptic transmission in the VTA.

#### Amplitudes of spontaneous miniature EPSCs were increased in dopaminergic neurons

To determine whether the increase in the field EPSP resulted from increased synaptic inputs onto dopaminergic neurons, we examined these neurons with whole-cell patch clamp recordings. Putative dopaminergic neurons were identified by their characteristic  $I_h$  (Johnson and North, 1992). Dopaminergic neurons are known to generate more than 40 pA of currents in response to hyperpolarizing voltage steps (Neuhoff et al., 2002) (Table 1). The frequency of spontaneous mEPSCs was not affected ( $P=0.22$ , *t*-test) (Fig. 3C). However, amplitudes of spontaneous mEPSCs of the putative dopaminergic neurons were significantly increased by EGF administration ( $P<0.01$ , *t*-test). Averaged cumulative histograms of inter-event intervals and amplitudes of mEPSCs also drew the same statistical conclusions ( $P>0.99$  for inter-event interval,  $P=0.0003$  for amplitude, K-S test) (Fig. 3D). In examining the passive electrical properties of recorded neurons, EGF-administration did not affect resting potential or input resistance whereas cell capacitance displayed a non-significant increase ( $P=0.07$ ) (Table 1). In contrast, EGF effects on mEPSCs of the  $I_h$ -negative neuronal population were insignificant or very limited (Fig. 4). The decreasing trend of the EGF-treated group in the frequency was insignificant in the parametric analysis ( $P=0.49$ , *t*-test) but significant in the nonparametric test ( $P=0.049$ , K-S test). Thus, these results, at least, suggest that postnatal EGF administration enhances sensitivity of the  $I_h$ -positive dopaminergic neurons to an excitatory neurotransmitter in mouse VTA.

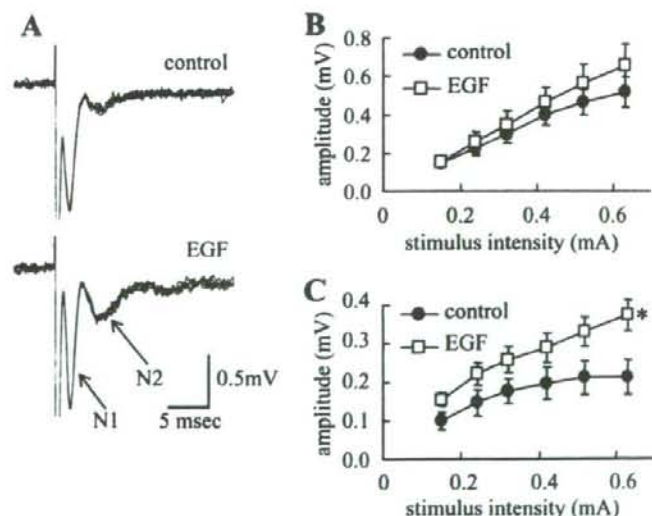


**Fig. 2.** Amplitude of the EPSP component of field potentials in the VTA. EGF (0.875  $\mu$ g/g s.c.) was injected daily into the neonatal mice from P2 to P15. Midbrain slices were prepared at P15–17 (A). Representative traces of field potentials recorded in horizontal slices. Two negative components that represent the fiber volley (N1) and synaptic potential (N2), were monitored in the presence of 20  $\mu$ M bicuculline (Zheng et al., 2006; Nugent et al., 2008). Five responses to electrical stimuli (0.62 mA) are superimposed for display. EGF administration increases the amplitude of the N2 component (C) without affecting the N1 component (B) (control:  $n=10$  slices from six animals; EGF:  $n=9$  slices from five animals). \*  $P<0.05$ , *t*-test.

Please cite this article in press as: Namba H, et al., Epidermal growth factor administered in the periphery influences excitatory synaptic inputs onto midbrain dopaminergic neurons in postnatal mice, *Neuroscience* (2008), doi: 10.1016/j.neuroscience.2008.10.057

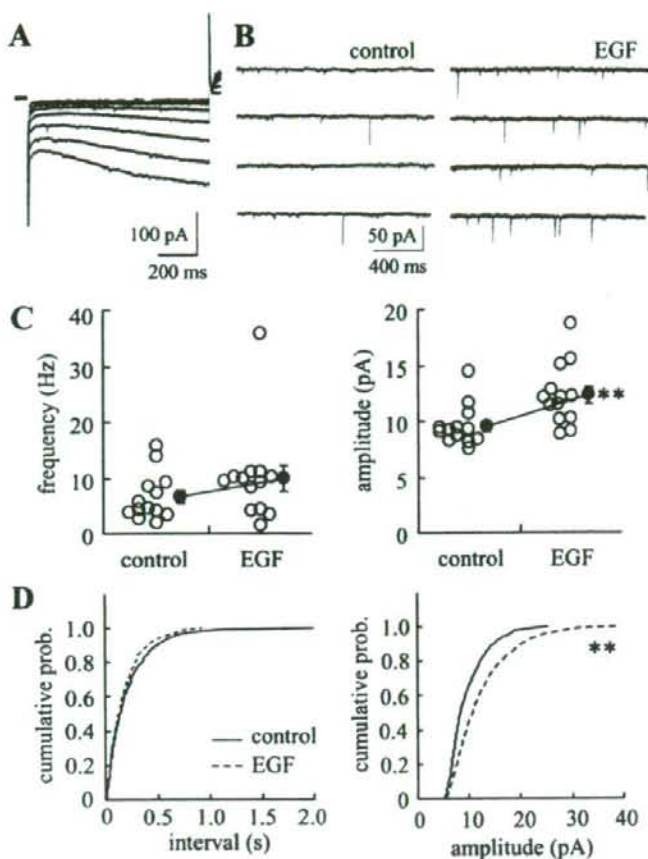


**Fig. 3.** Amplitudes and frequencies of mEPSCs in putative dopaminergic neurons. (A) Putative dopaminergic neurons were identified by their characteristic  $I_h$  (>40 pA). Hyperpolarizing voltage steps were applied with  $-10$  mV increments from  $-69$  mV to  $-139$  mV.  $I_h$ -positive neurons in the VTA were subjected to whole cell patch clamp recording. (B) Typical traces of mEPSCs for EGF-treated and vehicle-treated mice were displayed. (C) One hundred twenty miniature events were pooled and analyzed for each putative dopaminergic neuron. The mean amplitude and frequency of mEPSCs were calculated in each cell and plotted (control:  $n=13$  cells from seven animals; EGF:  $n=13$  cells from eight animals). \*\*  $P<0.001$ ,  $t$ -test. (D) Averaged cumulative histograms of inter-event intervals and amplitudes of mEPSCs were calculated and plotted with the same synaptic events for EGF-treated group and for saline-treated controls. \*\*  $P<0.001$ , K-S test.

To estimate the number of functional glutamate receptors at synapses of dopaminergic neurons, we determined the AMPA/NMDA ratio in the  $I_h$ -positive neurons (Fig. 5A). Excitatory synaptic currents were evoked by stimulating the anterior region of the VTA. Whole cell recording was carried out at different holding potentials in the presence of  $20 \mu\text{M}$  bicuculline. The AMPA/NMDA ratio was significantly increased in the  $I_h$ -positive dopaminergic neurons of EGF-administered animals ( $P=0.045$ ,  $t$ -test) (Fig. 5B). In addition, we measured the paired pulse ratio to assess alterations in presynaptic function. Consistent with the previous report (Bonci and Malenka, 1999), the majority of electrophysiologically identified dopaminergic neurons exhibited synaptic depression with paired pulse stimulation separated by 20–

100 ms intervals (control: six of seven cells; EGF: five of seven cells) (Fig. 5C). The paired pulse ratios were not affected by EGF administration ( $P=0.3$ ; two-way repeated measures ANOVA) (Fig. 5D). Therefore, EGF administration appeared to influence postsynaptic components rather than presynaptic function of the excitatory afferents to dopaminergic neurons.

#### EGF administration altered the expression of ionotropic glutamate receptors in the VTA

In the VTA, dopaminergic neurons express mRNAs for the AMPA-type glutamate receptor subunits GluR1 and GluR2/3 as well as the NMDA-type glutamate receptor subunits NR1, NR2A and NR2B (Paquet et al., 1997; Chen et al.,

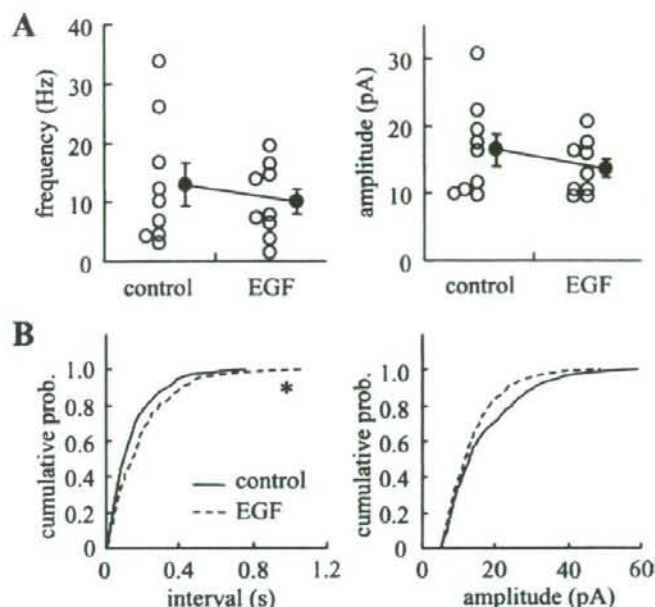


Fig. 4. Amplitudes and frequencies of mEPSCs in  $I_h$ -negative cells. One hundred twenty miniature events were pooled and analyzed for each  $I_h$ -negative cell. (A) The mean amplitude and frequency of mEPSCs were calculated in each cell and plotted (control:  $n=9$  cells from six animals; EGF:  $n=9$  cells from seven animals).  $t$ -test detected no significant differences. (B) Averaged cumulative histograms of inter-event intervals and amplitudes of mEPSCs were calculated and plotted with the same synaptic events for EGF-treated group and for saline-treated controls. \*  $P<0.05$ , K-S test.

2001; Yung, 1998). In contrast, the GluR4 AMPA receptor subunit is mainly expressed in neighboring GABAergic neurons (Paquet et al., 1997).

To examine the possibility that EGF administration influenced the expression of these glutamate receptor subunits, we determined the protein levels of AMPA and NMDA receptor subunits. Tissue containing the whole VTA and medial SNc was dissected from horizontal slices under a stereomicroscope and subjected to immunoblotting. We observed a statistically significant increase in the levels of the GluR1 subunit in animals receiving EGF ( $P=0.015$ ,  $t$ -test) (Fig. 6). GluR2/3 protein displayed a trend toward greater levels in EGF-treated animals, but did not reach statistical significance ( $P=0.067$ ). In contrast, GluR4 levels were not affected ( $P=0.35$ ). Protein levels of the NR1 NMDA receptor subunit were significantly elevated ( $P=0.030$ ), whereas NR2A and NR2B levels were not affected (NR2A,  $P=0.35$ ; NR2B,  $P=0.52$ ). In addition to the postsynaptic receptors, we examined the presynaptic markers synapsin I and synaptophysin. EGF administration had no effects on protein levels of these presynaptic molecules as well as a neuronal marker, NSE and an astrocyte marker, GFAP. These results suggest that synaptic potentiation following EGF administration might result from an increase in AMPA receptor expression in dopaminergic neurons.

## DISCUSSION

In the present study, we investigated subchronic influences of peripherally administered EGF on electrophysiological property of midbrain dopaminergic neurons in postnatal mice. Repeated administration of EGF enhanced excitatory synaptic transmission onto  $I_h$ -positive dopaminergic neurons in the VTA. Increases in the amplitude of mEPSCs and the AMPA/NMDA ratio were consistent with an increase in CNQX-sensitive potentials observed in field recording. In addition, we observed an elevation in the protein expression of the AMPA receptor subunit GluR1 and the NMDA receptor subunit NR1 in the ventral midbrain region. The elevation of glutamate receptor expression may underlie the increase in strength of synaptic inputs onto  $I_h$ -positive dopaminergic neurons.

In general, neurotrophic polypeptides exhibit distinct activities in acute and chronic phases (Patterson and Nawa, 1993). The acute effects mainly depend on intracellular signaling while chronic effects involve gene expression. Previous studies on hippocampal synaptic plasticity report the rapid synaptic responses to EGF. Acute application of EGF facilitates the induction of long term potentiation or enhances its magnitude (Ishiyama et al., 1991; Abe et al., 1991; Abe and Saito, 1992). Our preliminary study, however, indicated that acute EGF application to midbrain slice preparations failed to affect mEPSC (data not shown). Thus, the observed biological activity of EGF

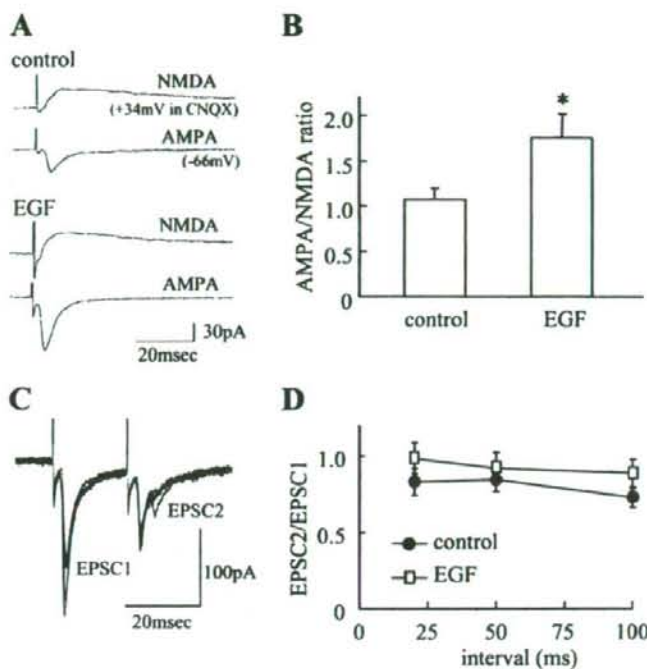


**Fig. 5.** Effects of EGF on the AMPA/NMDA ratio of EPSCs evoked in putative dopaminergic neurons. (A) Averaged traces for 10 synaptic responses are shown. Synaptic responses were triggered by electrical stimulation (0.05–0.2 mA, 0.067 Hz). AMPA currents were recorded at a holding potential of  $-66$  mV. NMDA currents were recorded at a holding potential of  $34$  mV in the presence of  $10 \mu\text{M}$  CNQX. (B) The AMPA/NMDA ratio was calculated for each cell and plotted as the means  $\pm$  S.E.M. (control:  $n=7$  cells from five animals; EGF,  $n=8$  cells from six animals). \*  $P<0.05$ ,  $t$ -test. (C) Typical responses of paired pulse inhibition of evoked EPSCs are shown for display. Four superimposed traces at the interval of  $20$  ms were recorded from control  $I_h$ -positive cells. Paired pulse ratios (peak amplitude of EPSC2/peak amplitude of EPSC1) were calculated from four averaged responses. (D) Paired pulse ratios at each stimulus interval ( $20$ ,  $50$ ,  $100$  ms) are calculated and plotted as the means  $\pm$  S.E.M. (control:  $n=7$  cells from five animals; EGF,  $n=7$  cells from four animals).

presumably represents the slow neurotrophic action of EGF that regulates dopaminergic development.

In our experimental paradigm, dopaminergic neurons were identified by their electrophysiological property of the  $I_h$  currents. The recorded cells were localized in the anterior region of VTA in the horizontal slices (Ford et al., 2006). Accumulated evidence suggests that, in this brain region,  $I_h$  currents serve as a specific electrophysiological marker for dopaminergic neurons as identified with tyrosine hydroxylase immunoreactivity (Ford et al., 2006; Neuhoff et al., 2002; Johnson and North, 1992; Wanat et al., 2008; but see also Margolis et al., 2006). In agreement, we also found that more than 70% of  $I_h$ -positive cells showed tyrosine hydroxylase immunoreactivity in post-fixed slice preparations (data not shown). Although we cannot fully rule out the possibility that some of the  $I_h$ -positive cells, in parts, represented non-dopaminergic cells (Margolis et al., 2006), it is likely that the  $I_h$ -positive cells not carrying tyrosine hydroxylase immunoreactivity were produced by cell dialysis of a patch pipette during recording. Thus, we considered that the electrophysiological property of  $I_h$ -pos-

itive cells mainly represents that of dopaminergic neurons in the VTA.

Whole cell recording revealed cell specificity of the postsynaptic action of EGF. Synaptic facilitation triggered by EGF was limited to the dopaminergic neurons exhibiting prominent  $I_h$  currents. No significant differences were detected in either the amplitude or frequency of mEPSCs in the  $I_h$ -negative neurons. In this context, immunoblotting might support the specificity of the neurotrophic effects of EGF on dopaminergic neurons. In the midbrain, mRNA and protein for GluR1, GluR2/3 and NR1 are detectable in tyrosine hydroxylase-positive dopaminergic neurons, whereas GluR4 is expressed only in GABAergic neurons (Paquet et al., 1997; Chen et al., 2001; Yung, 1998). The evidence that GluR4 levels were not affected in mice receiving subchronic administration of EGF may suggest insensitivity of the GABAergic population to EGF. In contrast, an influence of EGF stimulation on afferent fibers to midbrain dopaminergic neurons was relatively limited. Subchronic EGF administration did not influence mEPSC frequency or the paired pulse ratio in putative dopaminergic neurons. Furthermore,